INL/JOU-19-54399-Revision-0

Some observations of proposed criteria for "laminarization" in heated vertical tubes

Donald M McEligot, Xu Chu, Joong Hun Bae, Eckart Laurien, Jung Yul Yoo

September 2020

The INL is a U.S. Department of Energy National Laboratory
operated by Battelle Energy Alliance

INL/JOU-19-54399-Revision-0

Some observations of proposed criteria for "laminarization" in heated vertical tubes

Donald M McEligot, Xu Chu, Joong Hun Bae, Eckart Laurien, Jung Yul Yoo

September 2020

Idaho National Laboratory
Idaho Falls, Idaho 83415

http://www.inl.gov

Prepared for the
U.S. Department of Energy
Office of Nuclear Energy
Under DOE Idaho Operations Office
Contract DE-AC07-05ID14517

IJHMT paper HMT_2019_6643_R1
INL/JOU-19-54399

File = HMT_2019_6643_R1-ms.doc

26 May 2020

Discussion of previous papers by J.-i. Lee et al. [IJHMT 2008], Chu, Laurien and McEligot [IJHMT 2016] and McEligot et al. [IJHMT 2018]

DRAFT

Some observations concerning "laminarization" in heated vertical tubes

Donald M. McEligot[a,b,c], Xu Chu[d], Joong Hun Bae[e,1], Eckart Laurien[c] and Jung Yul Yoo[e]

[a] *Corresponding author*: Idaho National Laboratory, Idaho Falls, Ida. 83415-3850 USA
[b] Nuclear Engineering Div., Univ. Idaho, 1776 Science Center Drive, Idaho Falls, Ida. 83402 USA
[c] Institut für Kernenergetik und Energiesysteme, Uni. Stuttgart, Pfaffenwaldring 31, D-70569 Stuttgart/Vaihingen, Deutschland
[d] Institut für Thermodynamik der Luft- und Raumfahrt, Uni. Stuttgart, Pfaffenwaldring 31, D-70569 Stuttgart/Vaihingen, Deutschland
[e] Mechanical and Aerospace Engineering Dept., Seoul National Univ., 1 Gwanak-ro, Gwanak-gu, Seoul 08826, Korea

[1] Present address: Aerodynamics Group, Development Team #1, Koreanair R&D Center, Daejon 34054, Korea

Abstract

For low "turbulent" Reynolds numbers in strongly-heated vertical gas flow, fundamental results of existing direct numerical simulation (DNS) databases have been examined to deduce differences between cases which "revert" to turbulent and those that yield integral parameters which correspond to laminar flow (henceforth laminarizing or laminarized). Objectives are (1) to examine the streamwise evolution of near-wall flow structures and (2) to determine which, if any, proposed laminarization parameters could be used to discriminate between turbulent and laminarizing flows resulting. Views of streamlines in r- θ cross sections showed

evidence of a ring of irregular-shaped streamwise vortices near the wall at all locations. The transverse advection of these vortices is hypothesized to provide a path of least resistance to the transport of streamwise momentum in the wall-normal direction. It is demonstrated that a steady streamwise *laminar* vortex can provide *apparent turbulent* momentum transport (as a consequence of the Reynolds decomposition) such that a reasonable mean velocity profile is predicted near the wall. For the present cases, the values of the non-dimensional radius ($y_{c,w}^+ = Re_{\tau,w}$) and of the modified wall Reynolds number did discriminate whether turbulent or laminarizing flow resulted.

Key words: Vertical internal convective tube flow; variable gas properties; mixed convection; turbulent-to-laminar transition; laminarization; direct numerical simulation

Nomenclature

{ }	function of
<_>	mean or average value of
A	cross sectional flow area
c_p	specific heat at constant pressure
D	diameter; D_h, hydraulic diameter, $4A/\mathcal{p}$
G	mass flux, m/A
g	acceleration of gravity
h	convective heat transfer coefficient, $q_w" /(T_w - T_b)$
k	thermal conductivity
m	mass flow rate
ND	non-dimensional
p	pressure
$\mathcal{p}$	wetted perimeter
$q_w"$	convective heat flux from wall
R'	resistance to wall-normal transport of streamwise momentum per unit distance (depth), $(\partial U/\partial y)/\tau\{y\}$
r	radial coordinate
r_w	tube radius, D/2

s	spacing
T	temperature
U	streamwise mean velocity
u, v, w	velocities in streamwise, wall-normal and circumferential directions, respectively
u_τ	friction velocity, $(\tau_W/\rho)^{1/2}$
V_b	bulk velocity
W	width
x, y, z	coordinates in streamwise, wall-normal and circumferential directions, respectively

Non-dimensional quantities

Bo_J*	buoyancy parameter, $g\beta\, q_w" D^4/(k\nu^2 Re^{3.425} Pr^{0.8})$
C_f	skin friction coefficient, $2\,\tau_W/(\rho\, U_\infty{}^2)$ or $2\,\tau_W/(\rho\, V_b{}^2)$
D^+	diameter, Du_τ/ν
f	friction factor, $2\,\tau_W/(\rho V_b{}^2)$
Gr_{WS}	Grashof number in laminar analyses by Worsoe-Schmidt [IJHMT 1966], $g\, D^3/\nu^2$
K_a	acceleration parameter, eq. 4
K_B	buoyancy parameter, eq. 4
K_f	wall friction parameter, eq. 4
K_n	term in non-dimensional streamwise momentum equation, eq. 3
K_p	streamwise pressure gradient parameter, $(\nu/(\rho u_\tau{}^3))dp/dx = dp^+/dx^+$
K_V	acceleration parameter, $(\nu/V_b{}^2)(dV_b/dx)$
Nu	Nusselt number; Nu_D, based on diameter, hD/k
Pr	Prandtl number, $c_p\mu/k$
Q^+	convective heat flux, $q_w"\, r_w/(kT)$
q^+	convective heat flux, $q_w"/(Gc_pT)$
p^+	pressure, $p/(\rho\, u_\tau{}^2)$
R^+	resistance to wall-normal transport of streamwise momentum, $\mu R'$
Re	Reynolds number; Re_D, based on diameter, GD/μ; $Re_{W,m}$, modified wall Reynolds number, $V_b\, D/\nu_W$; Re_τ, based on friction velocity, $r_w\, u_\tau/\nu$; Re_θ, based on momentum thickness, $U_\infty\, \theta/\nu$
s^+	spacing, su_τ/ν
x^+	streamwise coordinate, xu_τ/ν
y^+	wall-normal coordinate, yu_τ/ν ; $y_c{}^+$, wall-normal coordinate at centerline; $y_V{}^+$,

	viscous layer thickness in two layer turbulence models [Prandtl, Phys.Z. 1910]; y_W^+ or $y\_,w^+$, based on properties evaluated at wall temperature
z^+	circumferential coordinate, zu_τ/ν
$\Delta_{p,w}$	streamwise pressure gradient parameter by Bankston [JHT 1970]
Δ_τ	shear-stress-gradient parameter [Patel and Head, JFM 1968], $\nu(\partial\tau/\partial y)_w/(\rho u_\tau^3)$
Λ	streamwise pressure gradient parameter by Narasimha and Sreenivasan [Adv.Appl.Math. 1979], $-(\delta/\tau_{w,in})dp/dx$; adapted for tubes, $= -(D/(2\tau_w))dp\{x\}/dx$
λ^+	wave length, $\lambda u_\tau/\nu$

Greek symbols

β	volumetric coefficient of expansion, $(-1/\rho)(\partial\rho/\partial T)_p$
δ	boundary layer thickness
θ	circumferential coordinate (angular); momentum thickness
κ	von Karman constant [ASME 1939]
λ	wave length
μ	absolute viscosity
ν	kinematic viscosity, μ/ρ
Π	geometric constant, 3.141593 approximately
ρ	density
τ	shear stress; τ_W, wall shear stress

Subscripts

b	evaluated at bulk temperature
c	centerline
D	based on tube diameter
eff	effective, i.e., laminar plus turbulent
i, in	inlet, thermal entry, x = 0
lam	laminar
n	index
th	thermal
turb	turbulent
w	wall; evaluated at wall temperature
∞	freestream

1. Introduction

Experiments to determine heat transfer characteristics of internal flows frequently employ a gas in a resistively heated vertical tube with an unheated entry for flow development [Lee et al., IJHMT 2008]. At low "turbulent" Reynolds numbers with "high" heating rates, results -- presented as graphs of local Nusselt number versus local Reynolds number -- show two characteristic shapes as in Figures 1a and 1b.; a comparable discrimination is shown by Bankston [JHT 1970] in terms of the Stanton number. Since viscosity increases with temperature, the bulk Reynolds number ($Re_b = GD/\mu_b$) decreases as the gas is heated, i.e., successive streamwise values move from right to left in the figures. Figure 1b was discussed in a recent note by McEligot et al. [IJHMT 2018]; the shape is hypothesized to occur when the viscous layer is thicker than the thermal boundary layer at the heated entry so that a laminar Leveque solution is reasonable. This situation is called "laminarization" [McEligot, Coon and Perkins, IJHMT 1970] or "deterioration" [Lee et al., IJHMT 2008]. In this note, we generally define the wall region as by Bradshaw [text 1971] with the region where molecular transport dominates called the "linear" layer and the region where it is noticeable called the viscous layer (to $y^+ \approx 30$ in unheated, high Re flows). However, when discussing the work of other investigators we may use their terminology.

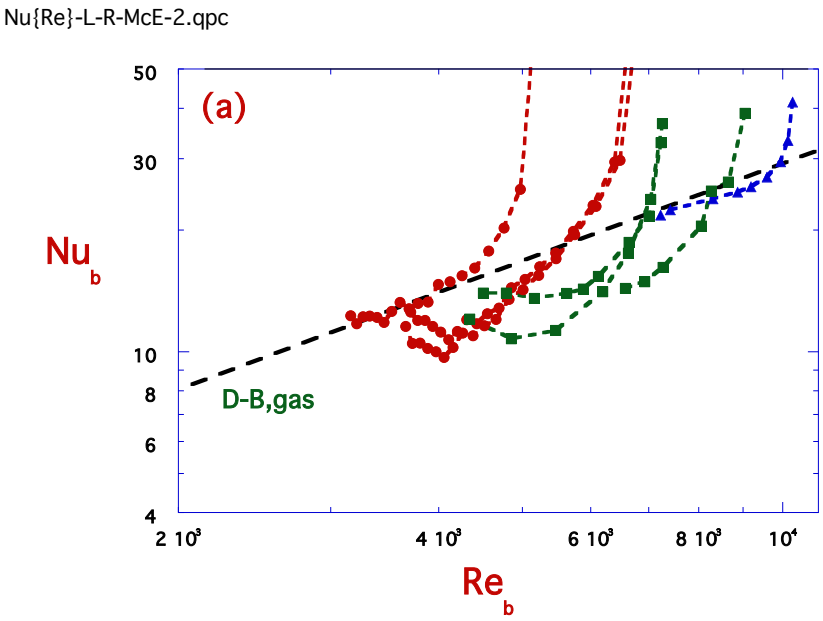

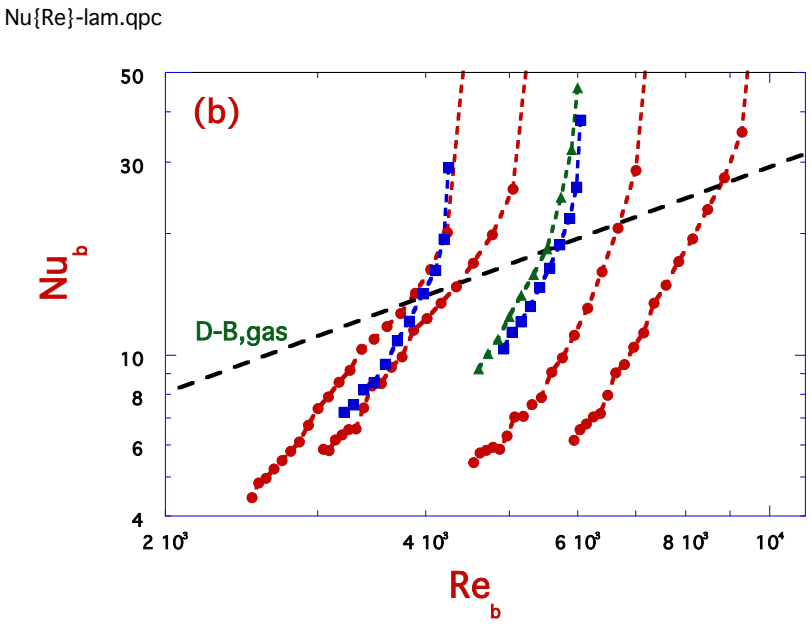

Fig. 1. Typical experimental results for internal convective heat transfer to gases at "low" Reynolds numbers with significant property variation. Dashed line = Dittus-Bölter correlation for gases [Drexel and McAdams, MIT TR 1945]. (a) Runs considered "turbulent," circles = Lee [MIT 2007], triangles = Reynolds [U. Arizona 1968], squares = McEligot [TID-19446], (b) runs considered "laminarizing," circles = Lee, triangles = Perkins [U. Arizona 1975] and squares = Shehata [U. Arizona 1984].

The trends demonstrated in Figure 1a occur when the flow can be considered to remain turbulent. Shown for comparison is the popular Dittus-Bölter correlation [U. Calif. 1930; Drexel and McAdams, MIT TR 1945]

$$Nu_b \approx 0.021\, Re_b^{0.8}\, Pr_b^{0.4} \qquad (1)$$

for fully-developed turbulent flow of gases in tubes with constant properties. For a given experimental run the high values in the figures represent results in the thermal entry where the termperature ratio $T_w\{x\}/T_b\{x\}$ increases with streamwise distance (and Re_b decreases). Further downstream the increase in T_b leads to $T_w\{x\}/T_b\{x\}$ decreasing. Typical empirical correlations

describing heat transfer with variable gas properties are ones like those of McEligot, Magee and Leppert [JHT 1965]

$$Nu_b \approx 0.021\, Re_b^{0.8}\, Pr_b^{0.4}\, (T_w/T_b)^{-1/2} \qquad (2)$$

for the downstream region and by Gnielinski [Int.Chem.Engr. 1976]. Beyond the thermal entry the effect of the variable gas properties (represented by T_w/T_b) is to reduce Nu_b below the Dittus-Bölter prediction. Then, as T_w/T_b decreases towards unity, Nu_b converges towards the correlation as seen in Figure 1a. For further background on effects of gas property variation on internal convective heat transfer, literature reviews in the papers by McEligot [Adv. Trans. Prop. 1986], Shehata and McEligot [IJHMT 1998], Bae et al. [Phys.Fl. 2006], Lee et al. [IJHMT 2008], Chu, Laurien and McEligot [IJHMT 2016], Valentin et al. [JHT 2018[and others may be helpful.

Comparing Figures 1a and 1b, one sees that --- at a given Reynolds number in this region --- a wide range in Nu (and therefore h) is possible so that predicted wall temperatures can be highly uncertain. A *general aim* of the present note is to reduce this uncertainty by examining proposed criteria that might discriminate between the likelihood of remaining turbulent or laminarizing. For that purpose we will employ direct numerical simulations (DNS) of the turbulent and laminarizing experiments of Shehata [U. Arizona, 1984; Shehata and McEligot, IJHMT 1998] and variations of his conditions.

The temporal three-dimensional DNS results provide much more information than just the integral parameters to address the above aim. For example, since the majority of the convective thermal resistance occurs in the viscous layers for low-Reynolds-number wall flows, it is appropriate to investigate the flow behavior there directly --- as can be done with the DNS results.

Useful reviews of studies of near-wall structure of turbulent boundary layer and duct flows have been provided by Kovasznay [AnRevFM 1970], Cantwell [AnRevFM 1981], Blackwelder [TPTF 1988], Robinson [AnRevFM 1991], Jimenez [Phys.Fl. 2013; JFM 2018],

Marusic and Monty [AnRevFM 2019], Tuckerman, Chantry and Barkley [AnRevFM 2020] and others. All treat incompressible flow with constant properties in contrast to the current cases with their strongly varying gas properties. The review by Robinson is still a valuable overview to various ideas on the near-wall structure of turbulent boundary layers and the one by Jimenez [JFM 2018] provides a detailed update with concentration on the coherent structures of all scales.

From his DNS Chu [IJHMT 2016] has presented a couple realizations of instantaneous streamwise cross-sections (r-x plane) for Shehata's Run 445 in his Figure 14: one at the thermal entry and the other showing the five diameters at the end of the tube. The latter shows so-called "streaks," one "low-speed" and one "high-speed" [Robinson, AnRevFM 1991; Jimenez, Phys.Fl. 2013] which are large relative to the diameter and persist along the entire sub-figure, i.e., 25-30 D. Bae [Phys.Fl. 2006] also provides instantaneous cross-sections in the r-x plane. He presents distributions of ρ and u at $22.5 < (x/D) < 25$ for four runs in his Figure 22. In his Figure 23 he also shows instantaneous isosurfaces near the wall for a constant value of the streamwise vorticity along the entire length of the tube, giving a clear demonstration of laminarizaton.

Consequently, the ***key objectives*** for the present study are (1) to examine the streamwise evolution of near-wall flow structures and (2) to determine which, if any, proposed laminarization parameters could be used to discriminate between turbulent and laminarizing flows resulting. These two objectives are not necessarily directly related.

2. Direct numerical simulations

As noted in our previous paper [McEligot et al., IJHMT 2018], experiments such as those by Lee [MIT 2007], Shehata [U. Arizona 1984] and others do not exactly replicate the desired idealizations of a step change in the wall heat flux nor the uniform wall heat flux in the heated section. Direct numerical simulations can match these idealizations more closely; in addition they can give more details on the turbulent flow and its temporal behavior than experiments usually can. So for closer representation of these thermal boundary conditions, we employ the DNS of J. H. Bae [Bae et al., Phys.Fl. 2006] and Chu [Chu, Laurien and McEligot, IJHMT 2016] modeling the experiments of Shehata [IJHMT 1998]. For constant properties, DNS results are

available at high Reynolds numbers in channels and tubes [Lee and Moser, JfM 2015; Satake et a., Fusion Sci.Tech. 2015] but laminarization in gaseous heat transfer tends to be a low-Reynolds-number, variable property phenomenon as present in all cases treated by Bae and Chu (except in the isothermal turbulence generating inlets). Studies of moderate-Reynolds-number turbulent catalytic combustion in a short channel with constant wall temperature have been performed with DNS by Arani et al. [Comb.Flame 2018]; they demonstrate some features like those in the investigations of Bae and Chu. DNS has also been applied to buoyant flows by He and colleagues [He, He and Seddighi, JFM 2016].

The numerical solver for DNS by Chu is based on low-Mach-number governing equations which are frequently employed in buoyant variable-density flow under low-Mach-number conditions such as strongly heated air flow [Bae et al., Phys.Fl. 2006; Chu, Laurien and McEligot, IJHMT 2016] or flow and heat transfer of supercritical fluids [Bae et al., Phys.Fl. 2008; Nemati et al. JFM 2016; Pandey, Chu and Laurien, IJHMT 2017;]. The governing equations are discretized with the open source finite-volume code OpenFOAM [Weller et al., Comp.Phys. 1998]. The Pressure-Implicit with Splitting of Operators (PISO) algorithm is applied for pressure–velocity coupling. The temporal term is discretized with a second-order implicit differencing scheme. The spatial discretization is handled with a central differencing scheme and a third-order upwind scheme (QUICK) is adopted for the convective term in the energy equation. The identical numerical solver has been frequently validated and used in our relevant previous research [Panley, Chu and Laurien, IJHMT 2017; Chu et al., IJHMT 2018].

Figure 1 by Chu, Laurien and McEligot [IJHMT 2016] shows the pipe geometry and boundary conditions. At the inlet, an inflow generator of a length of five diameters with an isothermal wall is adopted to generate approximately fully-developed inflow turbulence. A recycling/rescaling procedure is applied in this domain; it does not require any a priori knowledge of turbulent flow profiles. Bae et al. [Phys.Fl. 2006] used an a priori-conducted isothermal DNS to provide temporal inlet profiles. Both ways are frequently applied in high-fidelity DNS/LES as the inflow generator. Both Bae and Chu conducted validations with published databases to ensure proper fully-developed turbulence flowing into the thirty diameter heated sections. In the study by Chu, Laurien and McEligot [IJHMT 2016] the time-averaged

statistics in the heated region did not indicate any signature of periodicity from the inflow generator.

The cylindrical pipe model is constructed with a structured hexahedral mesh. The mesh resolution is approximately 115 x 120 x 240 (radial r, circumferential θ and axial x directions) for the inflow domain and 115 x 120 x 1440 for the heated domain. Compared with the resolution used by Bae et al. (69 x 129 x 769), approximately twice as many grid points are used in the radial and axial directions taking advantage of recent advances of high performance computation. For Chu's calculations the most coarse grid in wall coordinates was at the entrance in the higher Reynolds number cases where it was $\Delta x^+ \approx 8.2$, $\Delta y^+ \approx 0.17$ at the wall and $R\Delta\theta^+ \approx 10.3$; these values decreased in the downstream direction as the temperature and kinematic viscosity increased and the bulk Reynolds number Re_b decreased. For further details on these simulations, the reader is directed to their publications cited.

Both Bae and Chu treated the three upflow cases presented by Shehata with step changes to $q^+ = 0.0018$ (618U), 0.0035 (635U) and 0.0045 (445U). The close agreement of predicted $T_W\{x\}$, $Nu_b\{x\}$ and mean velocity and temperature profiles to experimental results validated Chu's DNS code; he also compared favorably to the Reynolds normal stress predictions of Eggels et al. [JFM 1994] for isothermal pipe flow. Eggels et al. proved that their mesh size satisfied the Kolmogorov length scale requirement; since Chu's spatial resolution was comparable to theirs, it is believed that Chu's mesh did as well. As the gas is heated in the downstream direction, the viscous length scale (ν/u_τ) increases so the spatial resolution improves further with x. Bae validated his DNS code with the same experimental data plus Shehata's streamwise mean pressure distributions. In addition Bae extended the conditions to include detailed predictions for non-buoyant idealizations (618F, 635F and 445F), two higher heating rates (455U and 455F) and one downflow (618D) while Chu added a non-buoyant version (445F) for the highest non-dimensional heating rate. We use some, but not all, of Bae's additional cases to supplement the four from Chu's more recent calculations.

The results presented in the present study are for Runs 618U, 635U, 445U and 445F by Chu and 618F, 618D and 635F by Bae. Inlet Re and q^+ of the DNS calculations are given later in Table 1 for Runs 618U, 635U and 445U while they are Run/Re_{in}/q^+_{in} = 618F/6000/0.0018, 618D/6000/0.0018, 635F/6000/0.0035 and 445F/4240/0.0047 for the others.

For this note, we operationally *define* a "laminarized" flow as one which has laminar values of integral parameters (such as convective heat transfer coefficient) when normally a reader would expect turbulent ones based on the local bulk Reynolds number. Likewise a "laminarizing" flow is one which differs from turbulent predictions and appears to be tending towards a "laminarized" flow. As shown in our earlier note [McEligot et al., IJHMT 2018], all three of Shehata's experiments agreed with a laminar thermal entry solution near the start of heating where the thermal boundary layer is thin relative to the molecular conduction layer; this behavior is expected for all turbulent flows when their velocity profiles are developed to some extent upstream of the start of heating. Thus, for these cases the labeling as "turbulent" or "laminarizing" tends to be based on the downstream evolution. The evolution of these layers is discussed in Section 4 of the earlier note including graphs of their development.

Two popular criteria have frequently been employed to predict whether a heated gas flow may laminarize or not; they employ an acceleration parameter and a buoyancy parameter or versions thereof. Acceleration is induced in an internal heated gas flow since the density decreases as the temperature increases so the integral continuity equation requires a streamwise increase in bulk velocity. Accordingly, the acceleration parameter for external turbulent boundary layers, $K_V = (\nu/V_b^2)dV_b/dx$, [Launder, MIT 1964; Moretti and Kays, IJHMT 1965; Kays text, pp. 96-7, 1966; Kline et al., JFM 1967] was converted to a thermal equivalent, $K_V \approx 4\ q^+/Re$ (a Reviewer recommends using K_t), for experiments in small heated tubes where buoyancy effects usually can be neglected [McEligot, Coon and Perkins, IJHMT 1970]. Thus, the 1963 flow regime map by McEligot [TID-19446] can be interpreted as showing that heated internal flows with $K_V > \sim 2 \times 10^{-6}$ can be expected to be "laminarizing" (called transitional at the time). A popular criterion for predicting laminarization/deterioration caused by buoyancy effects in

heated vertical gas flows uses the buoyancy parameter $Bo_J^* \approx g\beta_b q_w" D_h^4/(k_b \nu_b^2 Re_b^{3.425} Pr_b^{0.8})$ by Jackson, Cotton and Axcell [IJHFF 1989].

The brief review by McEligot and Jackson [NED 2004] mentions previous literature which recommends a range of values of K_V from 2×10^{-6} to 4×10^{-6} as possible criteria for expecting flow to laminarize. For his flows accelerated by lateral convergence, Murphy [JFM 1983] chose a threshold, $K_V < \sim 9.5 \times 10^{-7}$ where his data agreed with turbulent predictions. Likewise a five per cent threshold for buoyancy effects is $Bo_J^* > \sim 6 \times 10^{-7}$ and, in upflow, significant "deterioration" has been observed at $Bo_J^* > 8 \times 10^{-7}$ [Li, 1994].

Figures 2a and 2b show the streamwise variations of these two parameters for the present DNS results. Since K_V is primarily determined by the energy balance on the flow, for a given set of experimental conditions ("Run") the value of K_V does not depend on the direction or magnitude of gravity. Figure 2a shows that Runs 618U, 618F and 618D would be expected to be turbulent if acceleration were the only phenomenon (e.g., Runs 618F, 635F and 445F) while Runs 445U and 445F are in the range where laminarization would be forecast. Runs 635U and 635F vary from $K_V \approx 2.33 \times 10^{-6}$ at the entry to about 1.96×10^{-6} at the end of the domain so it would be considered uncertain (some investigators have suggested criteria as low as 2×10^{-6} to laminarize [McEligot and Jackson, NED 2004] but somewhat higher values are probably more common).

The evolution of the buoyancy parameter is shown in Figure 2b. For upflow $Bo_{J,b}^*$ decreases significantly in the downstream direction (i.e., up). For Run 445U, its value over the length of the test section is in the region where Jackson would predict laminarization ("deterioration") if acceleration were not already large enough. At the start of heating, Run 635U is in the range where laminarization would be expected but it decreases to the threshold by the end of the tube. Run 618U is below the value for significant deterioration throughout. Run 618D is in a range where Li and Jackson would predict slight enhancement (Figure 3 by McEligot and Jackson [NED 2004]). Runs 618F, 635F and 445F --- where buoyancy has been

suppressed --- should and do show zero for $Bo_{J,b}^*$, i.e., no buoyancy effects, consistent with our idealization for gas flow in small tubes.

Lee [MIT 2007] conducted related experiments in a longer tube, (L/D) ≈ 126, and examined the applicability of these two parameters for defining laminarization criteria. He found that, for his results, using local values for calculating the paraameters could be ambiguous but he concluded that by using inlet values he could successfully demarcate buoyancy-driven and acceleration-driven DTHT (Deteriorated Turbulent Heat Transfer) for tubes with uniform heat flux. For his data, he found that the values $K_{v,in} \approx 2.5 \times 10^{-6}$ and $Bo_{J,in}^* \approx 2 \times 10^{-6}$ and greater led to significant reductions in Nusselt number. For the present cases, these values would forecast that Run 445U would laminarize either due to acceleration or buoyancy and Runs 635U and 618U would remain turbulent.

In summary, Run 618U would be expected to remain turbulent, Run 445U to laminarize and Run 635U is somewhat uncertain. A ***pertinent question*** is how to forecast laminarization when both acceleration and buoyancy are significant, e.g., Run 635U.

Predicted local Nusselt numbers (dashed and dotted curves) are compared to the laminar Leveque solution [1928; Worsoe-Schmidt, IJHMT 1966] in Figure 3. Solid lines represent the Leveque solution for Re_{in} = 4240 and 6020 with the former being slightly lower since $(C_f Re)_{in}$ is less for it. Centerline markings show the variable property turbulent correlation of McEligot, Magee and Leppert [JHT 1965] for the downstream conditions.

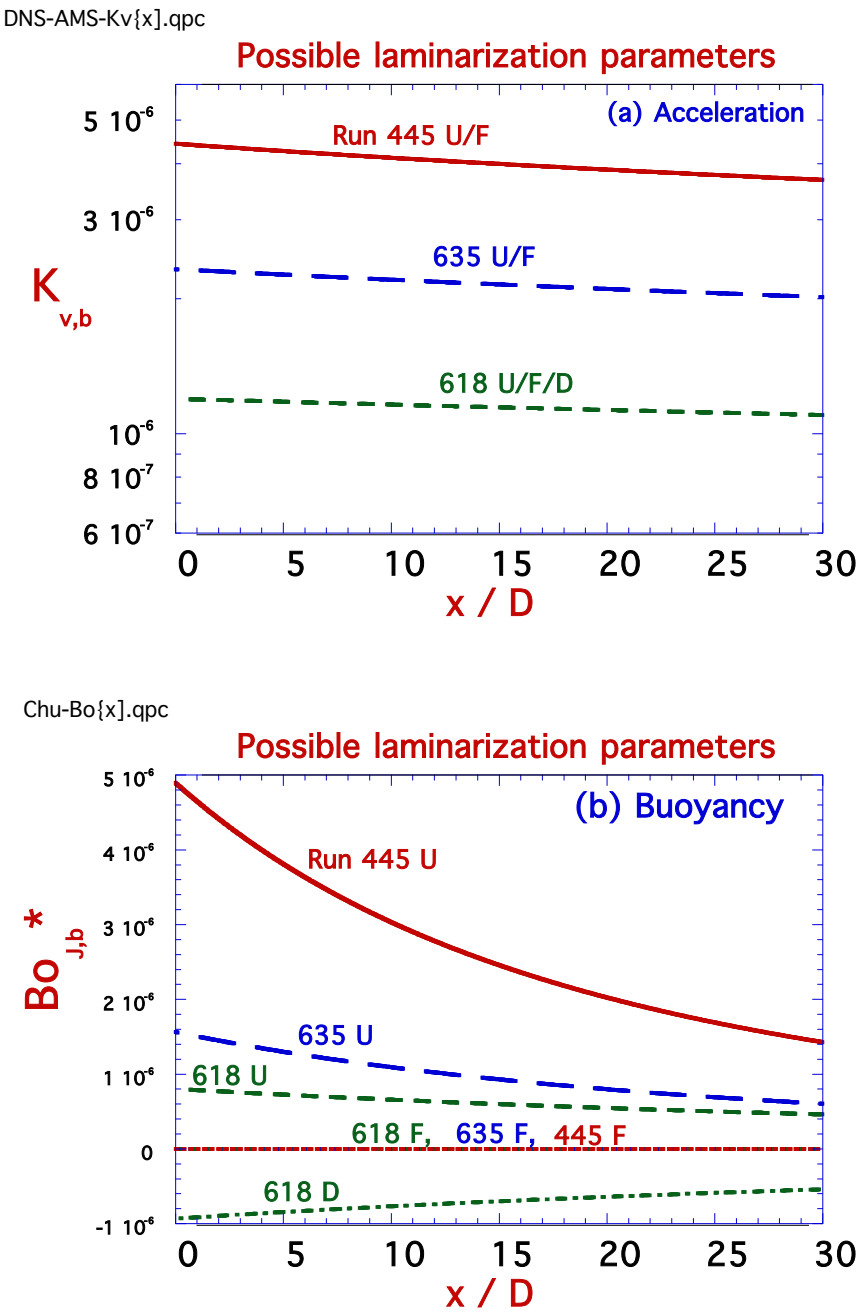

Fig. 2. Variation of possible laminarization parameters for conditions of Shehata's experiments from DNS of Bae [Bae et al., Phys.Fl. 2006] and Chu [Chu, Laurien and McEligot, IJHMT 2016].

Nu{x}-Lev-618U/F/D-semi.qpc

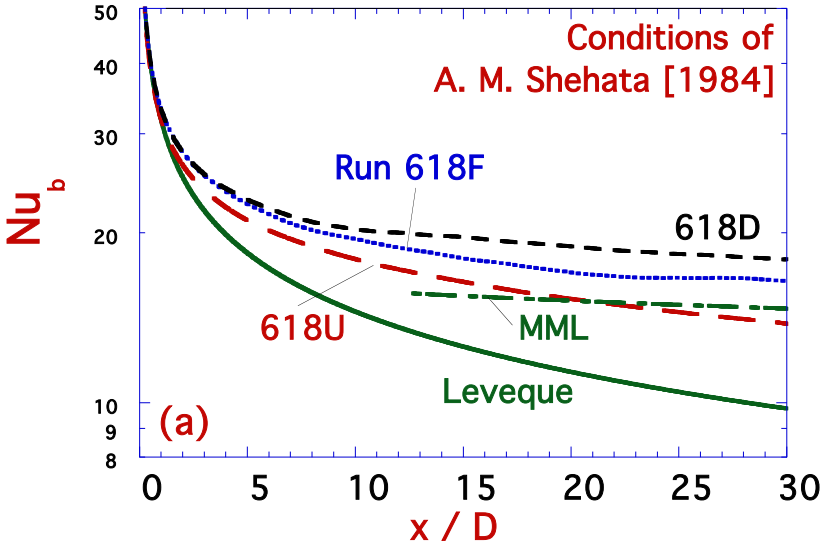

Nu{x}-Lev-635U/F-semi.qpc

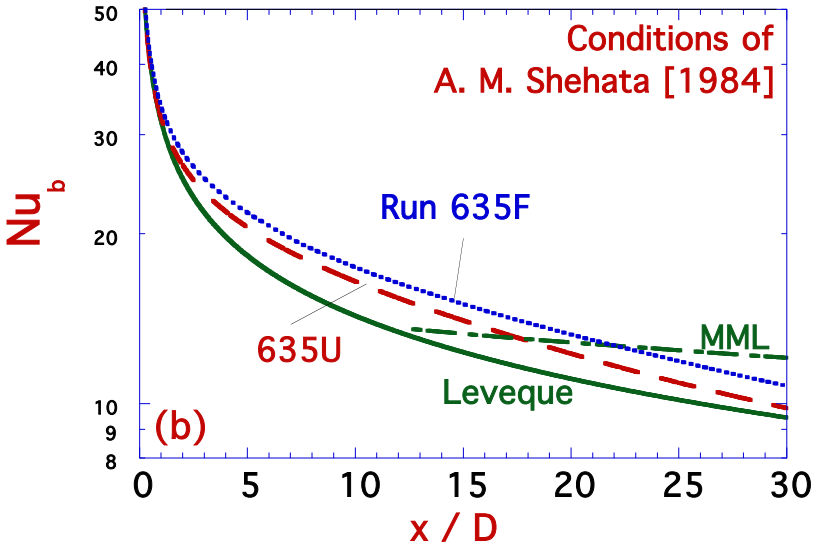

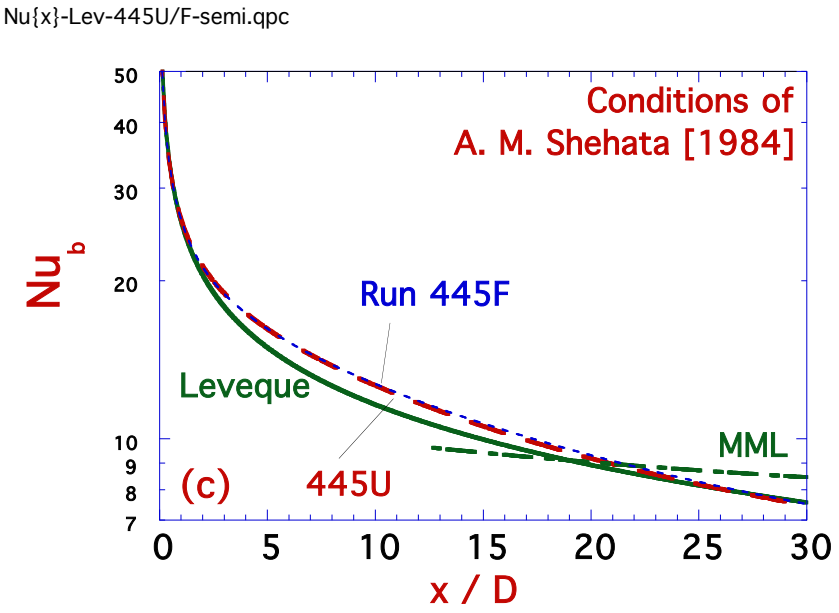

Fig. 3. Thermal entry predictions of convective heat transfer for the conditions of Shehata [U. Arizona 1984] by direct numerical simulation. (a) Run 618, (b) Run 635 and (c) Run 445.

The DNS prediction for Run 618U diverges from the Leveque relation at x/D ≈ 3 (Figure 3a). The downstream evolution of Run 618U is close to the correlation for turbulent variable-property heat transfer to gases in tubes by McEligot, Magee and Leppert; in accordance with our definition it is labeled "turbulent" rather than laminarizing. Comparison to Run 618F shows that Run 618U is affected by buoyancy forces, about twelve per cent at the end of the tube, and its Nusselt number is less than that of Run 618F. This observation is consistent with the predictions of Jackson's semi-empirical analysis for buoyancy effects in developed flow in vertical tubes (e.g., see solid curves in Figure 3 by McEligot and Jackson [NED 2004]; $Bo_{J,b}^{*} \approx 4.7 \times 10^{-7}$ shows about five per cent effect) but the magnitude is greater in the DNS. Likewise, the DNS predictions for the downflow case (618D) agree with the trends of Jackson's turbulent analysis; the Nusselt number is larger than without buoyancy (618F), i.e., "enhanced."

Predictions for the intermediate cases, Runs 635U and 635F, are presented in Figure 3b. One can see that both follow the laminar Leveque solution and appear to be converging towards it at the end of the simulated test section. Accordingly, we label both cases "laminarizing" and

note than Run 635F is predicted to laminarize from acceleration alone. Again one can see that buoyancy forces impede heat transfer in the upflow case in relation to pure forced convection. However, the difference from the Leveque prediction in the range ~5 < (x/D) < ~25 may imply that the convective heat transfer is assisted slightly by turbulent transport; that is, the convective thermal resistance is reduced slightly by some turbulent behavior.

The runs at the highest (non-dimensional) heating rate, 445U and 445F, agree closely with the laminar Leveque prediction *and with each other*. This latter observation can be taken as a clue that even without buoyancy the heating rate is sufficient to cause the flow to be laminarized; if so, the laminar thermal entry prediction of Worsoe-Schmidt [IJHMT 1966] could provide the appropriate comparison. Accordingly, we call both cases "laminarized." The buoyancy parameter in the upflow case ranges from about 5×10^{-6} to 1.5×10^{-6}; Jackson's analysis for it predicts a reduction from the forced convection Nusselt number of about fifteen to 45 per cent over this range (Figure 3 by McEligot and Jackson [NED 2004]). The non-dimensional parameters employed for laminar analyses are a heat flux parameter, $Q_{lam}^{+} = q_w" r_w/(kT)$, and a Grashof/Reynolds number ratio, $(Gr_{WS}/Re) = (g D^3/\nu^2)/(GD/\mu)$. For Run 445U their ranges are $7.1 > Q_{lam,b}^{+} > 3.2$ and $(Gr_{WS}/Re)_{in} < 165$, approximately. Figure 1 by Worsoe-Schmidt shows that for $Q_{lam}^{+} = 5$ and $(Gr_{WS}/Re)_{in} = 1000$ the maximum effect of buoyancy is less than 24 per cent in such laminar flows; for $(Gr_{WS}/Re)_{in} \approx 165$ we might expect about eight to ten per cent. A key difference between the analysis of Worsoe-Schmidt and the present DNS is the entering velocity profile: both are fully-developed but Worsoe-Schmidt used the parabolic laminar profile while the present idealization employed the turbulent profile of $Re_{in} = 4240$.

3. "Flow visualization" of near-wall structure

Additional insight into the evolution of Runs 618U, 635U and 445U can be obtained by examining the streamwise variation of the near-wall structure of their instantaneous fields, i.e., a computational version of photographic flow visualization. The DNS of these three runs involves heat transfer to a gas with significant variation of the fluid properties, except in the isothermal

turbulence generating inlet. On the other hand, in this present Section 3 the references cited generally involve isothermal flow and therefore constant fluid properties. For the present discussion, we select a different view from those of Bae and Chu mentioned in Section 1, instantaneous transverse cross-sections in the r-θ planes, Figures 4 and 5. Figure 4 provides contours of the streamwise velocity fields, instantaneous u{r,θ}, at three locations x = 5, 15 and 25 diameters for each of the three runs, 618U, 635U and 445U. In these figures blue represents low streamwise velocities, starting at zero at the wall, and dark red represents the highest velocities in the central region. Each sub-figure shows the streamwise evolution as the gas flow is heated, increasing the viscosity and reducing Re_b and $Re_{w,m}$ in the streamwise direction. Consequently, the viscous length scale increases in physical terms and the non-dimensional diameter and circumference decrease in wall units. Of particular interest to us will be the blue "bulges" from the wall towards the central core flow. These regions show lower streamwise speeds than the surrounding regions at the same radii. They identify what some other investigators call "low speed streaks" from early dye visualizations [Robinson, An.Rev.F.M. 1991]. Others might refer to them as "ejections" but this term means different things to different people and may or may not represent ejections as interpreted by Corino and Brodkey [JFM 1969]; so we will avoid this term. For convenience, we will generally call them simply "bulges." Also one can identify some dark red regions in the circumferential direction between the bulges so they represent higher speed flow than their surroundings at the same radii. Thus, these red regions could be what some investigators call "high-speed streaks" [Robinson, An.Rev.FM 1991] --- or possibly sweeps [Corino and Brodkey, 1969] or Bradshaw's "splats" [Wood thesis, 1980; Bradshaw and Koh, Phys.Fl. 1981]. Table 1 presents a few pertinent flow and geometric values for the three cases. In the downstream images for Runs 635U and 445U in Figure 4, some of the possible bulges were too weak to identify clearly in our manual counting so their numbers in Table 1 are marked as "?," meaning not known.

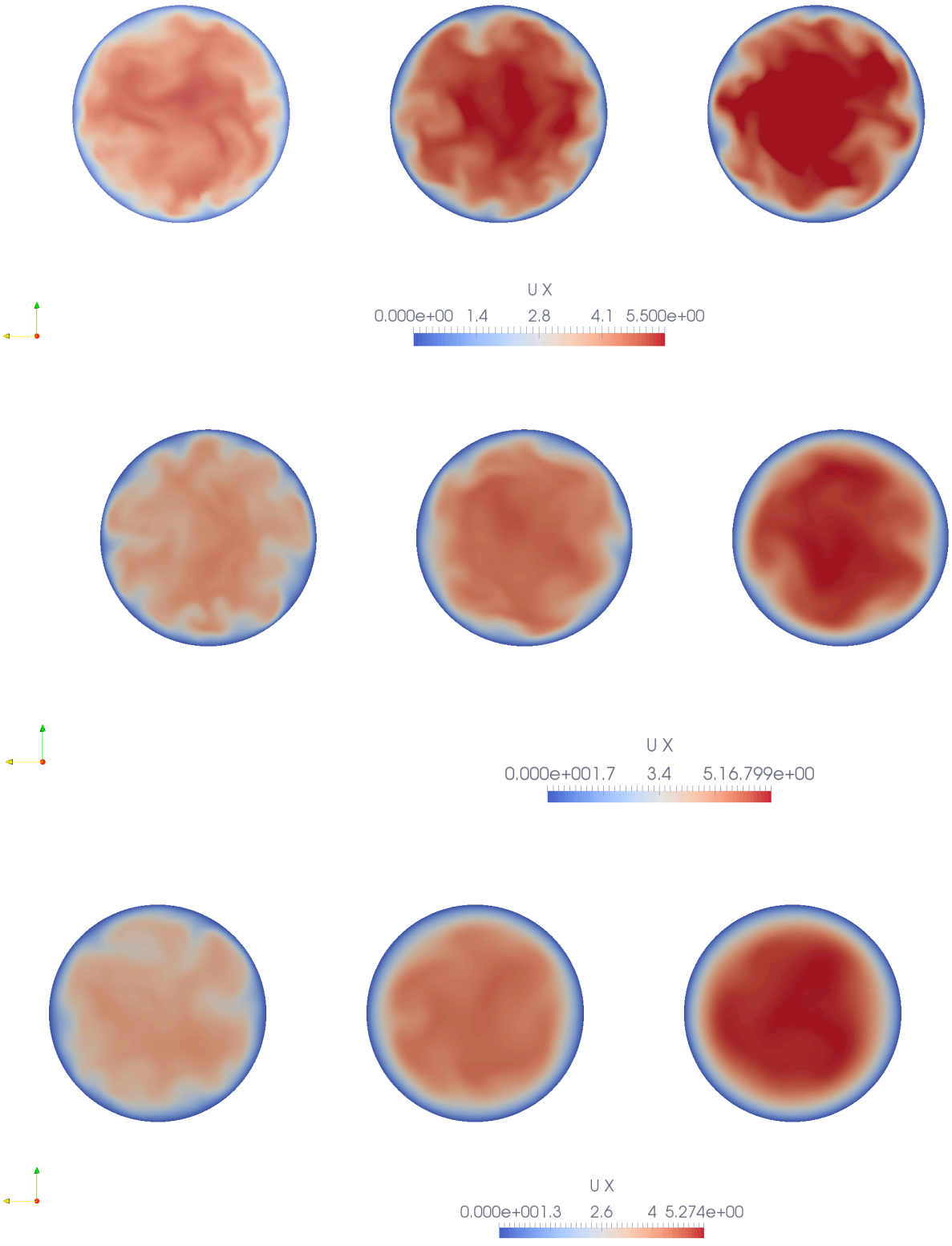

Fig. 4. Evolution of instantaneous streamwise velocities at cross-sections. Top = Run 618U, middle = Run 635U and bottom = Run 445U. Left to right: x = 5D, 15D and 25D.

Table 1. Geometric and flow values of cross-sectional views of instantaneous streamwise velocities (Figure 4).

x/D	Re_b	$Re_{w,m}$	$y_{c,w}^+$	Estimated "bulges"	Est. s_w^+
		Run 618U, Re_{in} = 6020, q^+_{in} = 0.0018			
5	5875	3573	140.7	13	68
15	5617	3222	126.8	13	61
25	5382	3074	119.7	12	62
		Run 635U, Re_{in} = 6020, q^+_{in} = 0.0035			
5	5760	2556	114	9	80
15	5320	2109	94	8	74
25	4958	1876	83	?	?
		Run 445U, Re_{in} = 4240, q^+_{in} = 0.0047			
5	3998	1588	83.8	9	58
15	3609	1285	68.2	7	61
25	3296	1162	61.5	?	?

Figure 4-top for Run 618U is a case considered to remain "turbulent." One sees a ring of low velocity gas along the wall, possibly corresponding to the so-called "laminar sublayer" where molecular transport dominates. Then at intervals circumferentially the low velocity extends away from the wall; these apparent bulges will appear in Reynolds-averaged statistics as negative fluctuations relative to the instantaneous average streamwise velocity at a given wall-normal distance y. In this run, one can estimate about twelve to thirteen bulges around the circumference. Thus, their average spacing s_W^+ is about 61-68 wall units (where the subscript

"w" indicates that it is based on properties at the wall temperature) in contrast to conventional estimates of about 100 in unheated turbulent flows [Robinson, An.Rev.FM 1991; Jimenez, Phy.Fl. 2013]. A comparable appearance is evident in the isothermal DNS predictions of Rudra et al. [Adv.Th.Hyd. 2018] but the spacing is larger, i.e., their Figure 3a.

Although Run 635U has the same entering Reynolds number as Run 618U, its appearance in these views (Figure 4-middle) is significantly different. To the eye the behavior of 635U could be described as less vigorous or smoother, particularly at 15D and 25D. Based on the local heat transfer results, this run was categorized as "laminarizing." While the number of low speed regions is fewer than in Run 618U and is observed to decrease from 5D to 25D as the non-dimensional circumference decreases, s_w^+ is slightly larger. Chu's Figures 9 and 10 show significant reductions in turbulence kinetic energy (TKE) and Reynolds shear stress at 14D and 25D compared to turbulent Run 618U [IJHMT 2016].

Laminarizing Run 445U with lower Re_{in} and higher q^+ continues the trends noticed for Run 635U: the flow pattern appears even less vigorous and smoother downstream (Figure 4bottom). At 15D the low-velocity bulges look less pronounced with less penetration into the central core. At 25D the instantaneous flow seems nearly axi-symmetric as in an idealized pure laminar pipe flow. These observations are consistent with Chu's Figures 9c and 10c where the TKE and Reynolds shear stress are low, approaching zero. At 5D and 15D the identifiable bulge spacing s_w^+ is about sixty.

Figure 5 shows streamlines formed from the instantaneous v and w fields for four locations, x = 0, 5, 15 and 25 diameters. The inlet at (x/D) = 0 represents a turbulent, fully-developed isothermal flow at the entering Reynolds number, Re_{in} = 6020 for two and 4240 for the highest heating rate. The next three show the evolution with heating at the same locations as in the previous Figure 4. For reference purposes, the locii where the mean value of y_w^+ equals thirty are identified by solid white circles. Following Bradshaw [text 1971], we consider the viscous layer to be the region near the wall where molecular transport is significant but not necessarily dominant; typically in isothermal flow it is to y^+ of about thirty (or more at low

turbulent Re like the present flows). So from the circles in Figure 5 one can see that the mean viscous layer occupies a significant portion of the cross-section in these low-Reynolds-number flows.

Fig. 5. Streamlines in cross-sectional planes (evolution of quasi-streamwise vortex patterns). Top = Run 618U, middle = Run 635U and bottom = Run 445U. Left to right: x = 0D, 5D, 15D and 25D. White solid circles denote the locii where the mean value of y_W^+ is thirty.

Each cross-section shows an irregular core flow surrounded by *a ring of irregular vortices near the wall*. (The core consists of high velocity flow as can be seen in Figure 4.) In these instantaneous cross-sections one sees an irregular "ring" of apparent vortex centers near the wall, approximately corresponding with our viscous layer. These centers are believed to indicate streamwise or quasi-streamwise vortices inducing "low-speed and high-speed streaks" at their circumferential sides. The ring of vortices scales approximately on the viscous layer --- or vice versa. The apparent vortices are of varying sizes, presumably relating to different stages in their individual lifetimes, and varying "strengths" (as evident from the penetrations of the corresponding low-speed blue bulges in Figure 4). The prevalence of these patterns leads us to

hypothesize that they form a fundamental structure of near-wall internal flow. That is, they appear to provide a key mechanism for accommodating the velocity difference between the central core and the no-slip wall.

One fundamental structure for internal circular tube flow is axi-symmetric laminar flow where transverse momentum transfer is purely via molecular transport. In our ***hypothesized second fundamental structure*** locally the advection of the vortices transfers x-momentum from the high velocity central region towards the zero velocity wall and from the low-velocity near-wall layer to the core. The vortices act somewhat like roller bearings. We suspect that, with turbulent flow, the pattern occurs when the conditions are such that the advection by the vortices represents a *path of least resistance* to and from the wall, i.e., less than the pure molecular shear flow. That is, the radially-directed flow of the vortices is believed to transport streamwise momentum in the wall-normal direction more easily than a near-laminar shear layer.

The transverse flow path of a quasi-streamwise vortex can be approximately described as (1) a flow away from the wall advecting the low streamwise velocity/momentum fluid from the immediate vicinity of the wall towards the central region (often described as a "low-speed streak" and the main emphasis of many investigators), (2) a circumferential flow adjacent to the central core where the low velocity fluid from the wall is accelerated to the higher velocity of the turbulent central core as in a free shear layer, (3) a wallward flow carrying high-velocity fluid typical of the central core (often identified as a "high-velocity streak") that impinges on the wall, raising the pressure at the stagnation line to provide forcing for a circumferential wall jet and (4) completing the path, flow along the wall as a wall shear layer or boundary layer decelerating the high-velocity fluid to velocities typical of the immediate wall region. In this immediate wall region, high indirect (turbulent) dissipation reduces the turbulent kinetic energy [Townsend, Camb.Soc. 1951; Rotta, Prog.Aero.Sci. 1962]. This streamwise process could persist if it is the optimal fundamental flow pattern based on a path of least resistance --- and thus could become the dominant "turbulent" flow pattern in this region.

This idea --- that of wall vortices forming a fundamental structure --- is comparable to, but a bit more specific than, that of Bejan [Walsh et al., ASME GT2006-91166] who indicates

that for any fluid flow system there are two possible architectures: (1) laminar shear flow and (2) streams (eddies, rolls, turbulence) in which momentum is transferred by organized fluid motion. The present hypothesis indicates that streamwise vortices form the important alternate architecture, giving a path of lower resistance than molecular shear.

The approximate centers of the vortices were estimated visually on copies of the subfigures as being in the middle of their smallest closed streamlines. "Height" was then estimated by selecting the streamline that was closest to the centerline and still apparently belonged with the identified vortex. These values were estimated visually by comparison to the reference circle.

The centers of the vortices in this ring (or layer) fall in a range of $y_w^+ \approx 5$ to ~ 35. The lower values correspond to smaller vortices which we suspect are in initial stages of their growth. The maximum "heights" of the larger vortices are of the order of $y_w^+ \approx 50\text{-}60$. The irregular pattern could partially be caused by random disturbances from upstream, possibly from instabilities of an entrance separation bubble or --- in the present case --- a developed turbulent flow upstream. The distorted cross sections of the vortices are likely caused by interactions with other structures in the vicinity.

Figure 5-top presents the instantaneous transverse streamline patterns for turbulent Run 618U. From the white circles one can see that the nominal mean viscous layer thickens slightly in the downstream direction as the Reynolds number decreases due to heating the gas. Accordingly, the number of vortex centers identified by eye in the near-wall ring decreases slightly, from about nineteen to seventeen. Correspondingly, Chu's plots show only slight variations in mean TKE and Reynolds shear stress.

Laminarizing Run 635U shows significant thickening of the mean viscous layer in the streamwise direction with a corresponding reduction in the number of identified vortex centers from nineteen to about eleven. By 25D the mean viscous layer reaches about one third of the radius and only a few vortex patterns are evident in the central core.

Run 445U starts at a lower Re_{in} than the other two runs and, therefore, has fewer apparent vortices in the near-wall ring at the entry --- about sixteen (Figure 5-bottom). By 5D the mean viscous layer has grown to about one-third of the radius with about twelve identified vortex centers in the ring. By the last station at 25D, the mean viscous layer reaches about halfway to the centerline and there are five to six vortex centers, depending how one counts. Despite these distinct vortices, they must be very weak with low wall-normal velocities since the corresponding view in Figure 4-bottom shows no significant inward bulge. As noted earlier, Chu's plots showed near zero TKE and Reynolds shear stress at this station. And as shown by Figure 3c, this run agreed closely with the predictions of the laminar Leveque theory, an observation consistent with the estimate by McEligot et al. [IJHMT 2018] that the entry thermal boundary layer mostly remained within about one-third of the radius (their Figure 4c). *So at this station the vortex structure persists but molecular transport dominates rather than the vortex advection.*

One might ask --- in experiments and DNS, why are pointwise values unsteady and apparently turbulent ? One of a number of possible explanations is that the motion of the vortices themselves, as the flow proceeds downstream, may carry the varying velocity distribution across a stationary probe or a fixed point. Examination of a time-series of x-θ images for Run 618U at $y_w^+ \approx 35$ near x/D = 15 (not shown) demonstrates that, in addition to being highly irregular in shape, most vortices have axes that form a slight angle with the downstream direction (tube axis). Following a few distinctive features on low-velocity streaks, one can deduce a circumferential motion of the associated vortex of about two-thirds of a typical vortex radius as the structure moves 500 wall units downstream.

The evolution of the vortex pattern is described in Figure 6 in terms of the number of vortices identified around the tube circumference. For $Re_{w,m} > \sim 3000$ the number of vortices does not vary significantly despite some scatter related to the difficulty of counting manually; this observation implies that --- in this range --- the spacing of the vortex centers increases gradually with $Re_{w,m}$, consistent with the "low-velocity-bulge" spacing in Table 1. At some $Re_{w,m}$ above the present range the vortex spacing may approach an asymptotic value (~50?) as

the viscous sublayer becomes thin relative to the tube radius. Below $Re_{w,m} \approx 3000$ the number of vortices decreases approximately logarithmically with $Re_{w,m}$, possibly towards an asymptote of two or zero. This decrease corresponds to the increase of the viscous layer thickness in physical terms (and the accompanying decrease of the circumference in wall units).

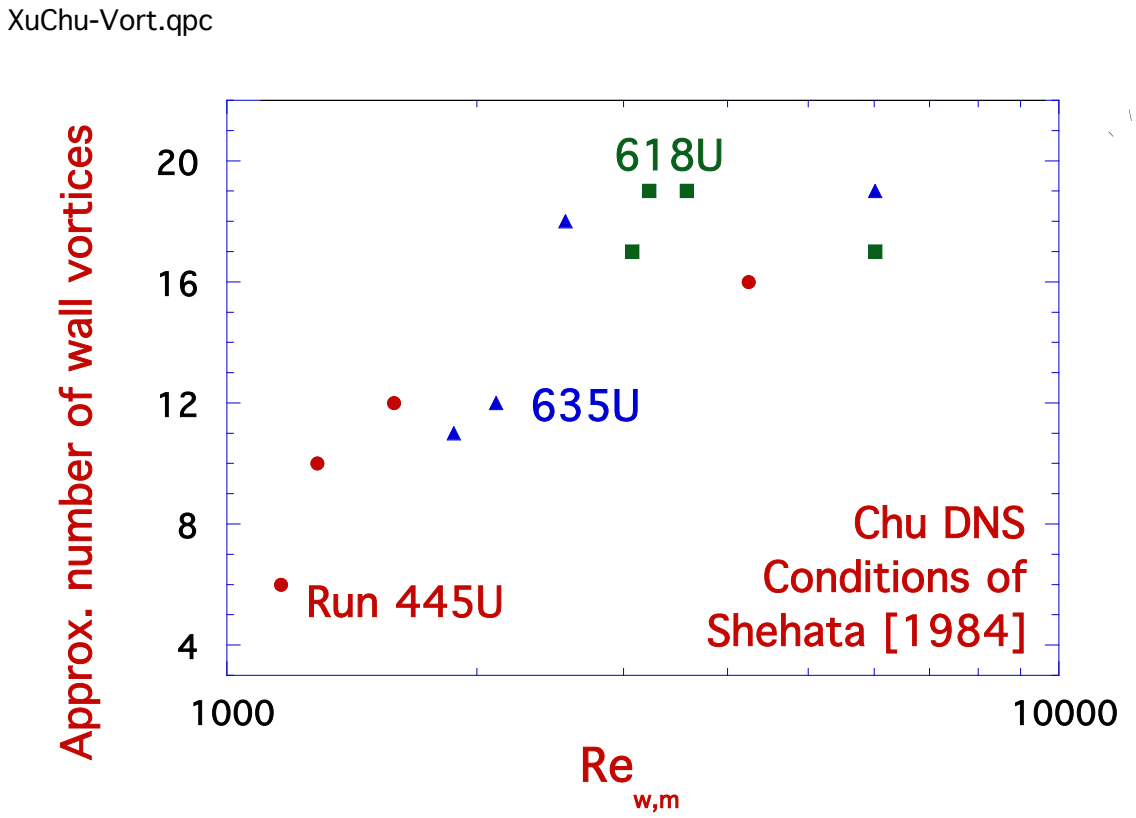

Fig. 6. Variation of number of identified vortices around circumference of tube (modified wall Reynolds number decreases in the downstream direction). Run 618U = squares, Run 635U = triangles and Run 445U = circles.

4. Potential criteria

In the past, stability analyses have been applied to the problem of transition from laminar to turbulent boundary layers to account for various stabilizing/destabilizing phenomena [Schlichting 7]. For example, favorable streamwise pressure gradients associated with flow acceleration have been found to delay transition of a boundary layer, a heated wall is believed to

destabilize a gas flow [Mack, Schlichting 7 1979, XVIIe] and vertical free convection can produce strong destabilizing effects [Nachtsheim, NASA TN D-2089, 1963]. Narasimha and Sreenivasan mention [p 246, Adv. Appl. Mech., 1979] that Schubauer and Skramstad [1947] and Liepmann [1943, 1945] observed that incipient turbulence could be suppressed by a favorable pressure gradient. Likewise, several phenomena have been suggested as causing "laminarization" of turbulent flows and potential critical parameters have been identified [Narasimha and Sreenivasan, 1979; McE and Jackson, NED 2004]. Narasimha and Sreenivasan [Adv. Appl. Mech., 1979] provided an excellent, useful review of the status of research into laminarization of fluid flow to the late 1970s. As noted by Narasimha and Sreenivasan [p 248, Adv. Appl. Mech., 1979], for recognizing the onset of laminarization different techniques have bee applied by different workers and as criteria for the occurrence of retransition they have suggested different parameters.

Parameters for two of the most popular criteria for laminarization have been discussed above in our section on "Direct Numerical Simulations:" a thermal acceleration parameter, K_V, [McEligot, Coon and Perkins, IJHMT 1970] and a buoyancy parameter, Bo_J^* [Jackson, Cotton and Axcell, IJHFF 1989]. For the cases considered both have significant magnitudes (except Runs xxxF) so the question of coupled effects is pertinent. The flow regimes of the DNS results for Runs 618U/F/D and 445U/F agree with the forecasts based on these parameters. Runs 635U/F were forecast to be "uncertain" and the DNS predictions indicate that they would laminarize.

As mentioned earlier, Lee [MIT 2007] recommends using inlet values to evaluate K_V and Bo_J^* from his experiment with a long tube having a uniform heat flux. In the hope of being useful for conditions with varying $q_W"\{x\}$ as well as Shehata's shorter test section, the present study examines most parameters in terms of local values.

Patel and Head [JFM 1968] indicate that they expect a fully turbulent flow to revert to laminar when its shear-stress-gradient parameter $\Delta_\tau = \nu(\partial\tau/\partial y)_w/(\rho\, u_\tau^3) = -1/y_c^+$ (in fully-developed flow with constant properties) is -0.009 or less (i.e., $|-\Delta_\tau| > 0.009$) . In terms of a

pressure gradient parameter K_p, (= $(\nu/(\rho u_\tau^3))$ dp/dx) Spalart [JFM 1986] found he could simulate a turbulent boundary layer at $(-K_p) \approx 0.02$ but could not at a Reynolds number corresponding to $(-K_p) \approx 0.025$ [McE and Eckelmann, JFM 2006]; this observation may be taken as an indication of likely laminarization. For heated turbulent gas flow in a circular tube, Bankston [JHT 1970] suggested that when $(-K_{p,w}) > \sim 0.02$ transition to laminar flow is likely to be initiated; the subscript "w" indicates evaluation of ν and ρ at the local wall temperature.

Narasimha and Sreenivasan [p 254, Adv. Appl. Mech., 1979] formulated a "quasi-laminar" description of evolution during reversion of an accelerated turbulent boundary layer in terms of another pressure gradient parameter, $\Lambda = - (\delta/\tau_{w,in})$ dp/dx, where δ is the boundary layer thickness and $\tau_{w,in}$ is the wall shear stress just before the pressure gradient is applied. This parameter may be derived from a streamwise momentum equation as a non-dimensional ratio of the pressure gradient term to a turbulent shear stress term; large values of Λ allow neglecting the latter. They show excellent agreement of their quasi-laminar theory compared to the $C_f\{x\}$ measurements of Blackwelder and Kovasznay [1972] when Λ exceeds about fifty, i.e., during the apparent relaminarization. From this comparison, on their page 256 they conclude that, in spite of the highly disturbed state of the flow, the strong stabilizing influence of a favorable pressure gradient can maintain an effectively laminar inner layer.

For a pipe flow, we estimate the effective boundary layer δ as D/2 and use V_b as the characteristic velocity so the pressure gradient parameter of Narasimha and Sreenivasan [Adv. Appl. Mech., 1979] may be recast as $\Lambda = - (D/(2\tau_w))$ dp{x}/dx or, for isothermal flows where Re_D is constant, $\Lambda = (Re_D/2)(C_f/2)^{½}(-K_p)$. With gas property variation we can evaluate the wall shear stress as Narasimha and Sreenivasan do at the origin of the effect (the start of heating in our case), $\tau_W = \tau_{W,in}$ for Λ_i, or evaluate it locally, $\tau_W = \tau_{W,b}$ for $\Lambda_b\{x\}$. The two are plotted in Figure 7. Although one might prefer a local description, Figure 7a demonstrates that it is not helpful as a criterion for laminarization in these cases. One cannot choose a value of $\Lambda_b\{x\}$ which discriminates between a turbulent or laminarizing result.

For the present DNS cases, Λ_i is more useful than $\Lambda_b\{x\}$ for discriminating between laminarizing and remaining turbulent as shown by Figure 7b. For $\Lambda_i < \sim 4$ the predictions remain turbulent and for $\Lambda_i > \sim 6$ they laminarize. However, between these two values Λ_i does not provide a definitive criterion; for example, turbulent Run 618U has a higher value of $\Lambda_i\{x\}$ than laminarizing Run 635F. Consequently, in the range $4 < \Lambda_i < 6$, the resulting flow regime is uncertain (and the cautious analyst probably should choose the worst case for the situation analyzed). It is not clear to us why the magnitude of the laminarizing value of Λ_i is significantly lower than that of Narasimha and Sreenivasan [Adv. Appl. Mech., 1979]; some possibilities are the considerable difference in the geometries, use of V_b instead of U_∞ in the definition and additional effects of tubular wall friction and, in some cases, buoyancy in the momentum equation.

As a possible answer to the earlier question of how to forecast laminarization when both acceleration and buoyancy are significant, e.g., Run 635U, we can extend Ezato's guidance [JHT 1999]. Lee [Correlations IJHMT 2008] has suggested that the parameter $q^+/Re^{0.44}$ could capture both effects but this overlapping regime was not covered in his data; however, this parameter depends on the tube diameter and gas. Ezato has shown the relative importance of acceleration, wall friction and buoyancy in Shehata's experiment in terms of the one-dimensional streamwise momentum equation (his equation 15). By employing their various definitions, one can cast this equation as a relation between some of the above parameters to give a pressure gradient parameter based on wall coordinates,

$$- K_{p,w}^+ = - (\nu_W/(\rho_W u_\tau^3))\, dp/dx = \Sigma K_{n,w}^+ \quad \text{where } n = a, f, B$$
$$= K_{a,w}^+ + K_{f,w}^+ +/- K_{B,w}^+ \qquad (3)$$

The three right hand terms represent acceleration, wall friction and buoyancy, respectively. Here the subscript w indicates evaluation of properties at the wall temperature and the plus sign of the buoyancy term applies for upflow. The individual terms can be represented as

Chu-Lambda{x]-2.qpc

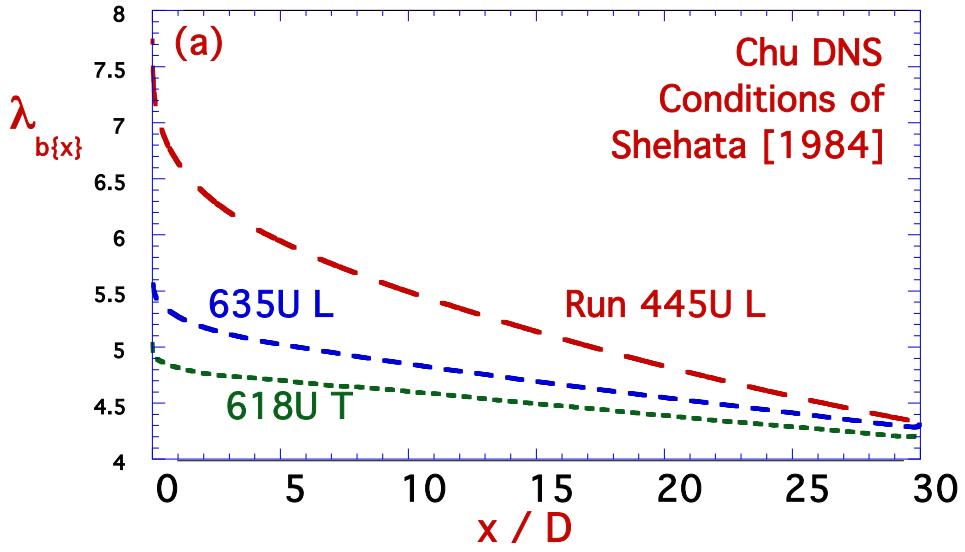

DNS-AMS-lambda{x}.qpc

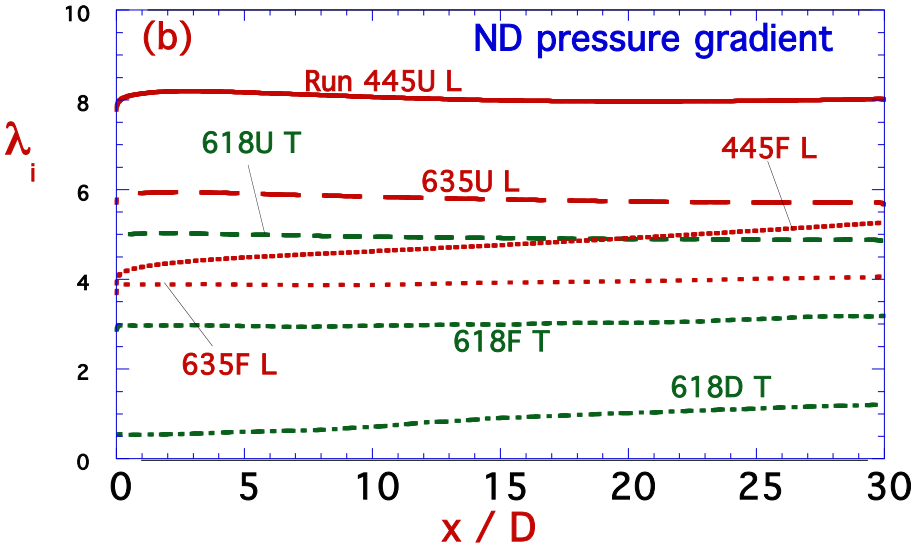

Fig. 7. Examination of possibility of using modified Narasimha-Sreenivasan pressure gradient parameter Λ as a criterion to forecast laminarization or turbulent flow: (a) $\Lambda_{b\{x\}}$, based on local wall shear stress, and (b) Λ_i, based on initial wall shear stress as by Narasimha and Sreenivasan [Adv. Appl. Mech., 1979]. ND = non-dimensional.

$$K_{p,w}^{+} = dp_w^{+}/dx_w^{+}$$

$$K_{a,w}^{+} = (\rho_b/\rho_w)\, V_{b,w}^{+}\, dV_{b,w}^{+}/dx_w^{+}$$

$$K_{f,w}^{+} = 4 / D_w^{+} \qquad (4)$$

$$K_{B,w}^{+} = (\rho_b/\rho_w)\, Gr_{WS,w} / (D_w^{+})^3$$

$$\text{with } Gr_{WS,w} = g\, D^3 / \nu_w^2$$

The pressure gradient parameter $K_{p,w}^{+}$ can be seen to be the same as the parameter $\Delta_{p,w}$ Bankston uses for his criterion [JHT 1970].

The familiar acceleration and buoyancy parameters [Launder, 1964; Jackson, Cotton and Axcell, IJHFF 1989] can be related to these versions in wall coordinates. The acceleration term can be expressed as

$$K_{a,w}^{+} = (\mu_w/\mu_b)\ (\rho_b/\rho_w)^{1/2}\, K_{v,b} / (C_{f,b}/2)^{3/2}$$

Likewise, the buoyancy term can be evaluated from Jackson's buoyancy parameter as

$$K_{B,w}^{+} = (\rho_b/\rho_w)\, (\nu_b/\nu_w)^2\, Bo_{J,b}^{*}\, Re_b^{3.425}\, Pr_b^{0.8} / [2\, Q_b^{+}\, (D_w^{+})^3]$$

The friction term may be written as $2/y_{c,w}^{+}$ or $2/Re_{\tau,w}^{+}$. Approximate inlet values of the terms in equation (3) are listed in Table 2 for runs considered in this note. These DNS results provide local predictions of $C_f\{x\}$ at each step and they should be reasonably accurate. The column "R" is our estimation of the flow regime by comparison to the laminar Leveque prediction and a downstream turbulent correlation as in Figure 3; L indicates laminarizing and T means apparently reverting to or remaining turbulent.

From the DNS predictions of Chu, the streamwise evolutions of the terms in $K_{p,w}^{+}$ are graphed in Figure 8a for Run 635U; the trends for Runs 618U and 445U are the same (not shown). As the local Reynolds number decreases with x so does $y_{c,w}^{+}$ leading to an increase of $K_{f,w}^{+}\{x\}$ and it becomes largest downstream. The acceleration contribution $K_{a,w}^{+}$ is approximately constant and is the smallest of the three terms for these runs. The buoyancy term $K_{B,w}^{+}\{x\}$ decreases with x, countering the increase of $K_{f,w}^{+}\{x\}$ to some extent. At the inlet,

for Run 618U the acceleration, friction and buoyancy terms contribute about 16, 40 and 45 per cent of the pressure gradient parameter, respectively. They yield 27, 35 and 45 per cent for Run 635U and 24, 26 and 50 per cent for Run 445U. So buoyancy is the largest contributor at the entry in these runs. These contributions are consistent with the observations of Bae [Phys. Fluids 2006] who employed a different non-dimensional definition for the pressure gradient.

Table 2. Approximate inlet pressure gradient parameters for cases considered.

Run	Author	Re_{in}	R	$K_{a,in}^+$	$K_{f,in}^+$	$K_{B,in}^+$	$-K_{p,in}^+$	Λ_{in}
618U	Chu	6020	T	0.00396	0.00991	0.01063	0.02450	4.95
618F	Bae	6000	T	0.00385	0.00983	0.0	0.01368	2.78
618D	Bae	6000	T	0.00385	0.00983	-0.01195	0.00172	0.35
635U	Chu	6020	L	0.00770	0.00991	0.01063	0.02824	5.70
635F	Bae	6000	L	0.00748	0.00983	0.0	0.01731	3.52
445U	Chu	4240	L	0.01254	0.01334	0.02597	0.05186	7.77
445F	Chu	4240	L	0.01254	0.01334	0.0	0.02580	3.88

Figure 8b compares the evolutions of $(-K_{p,w}^+)$ for the seven cases of Table 2. One sees that for $(-K_{p,w}^+)$ less than 0.02 the predictions remain turbulent and for $(-K_{p,w}^+)$ greater than 0.04 they have been classified as laminarizing. However, as with the Narasimha-Sreenivasan pressure gradient parameter, this parameter does not discriminate in an intermediate range, $0.02 < (-K_{p,w}^+) < 0.04$ for this set; laminarizing Run 635F and turbulent Run 618U overlap in this range so the value of $(-K_{p,w}^+)$ is an uncertain criterion there.

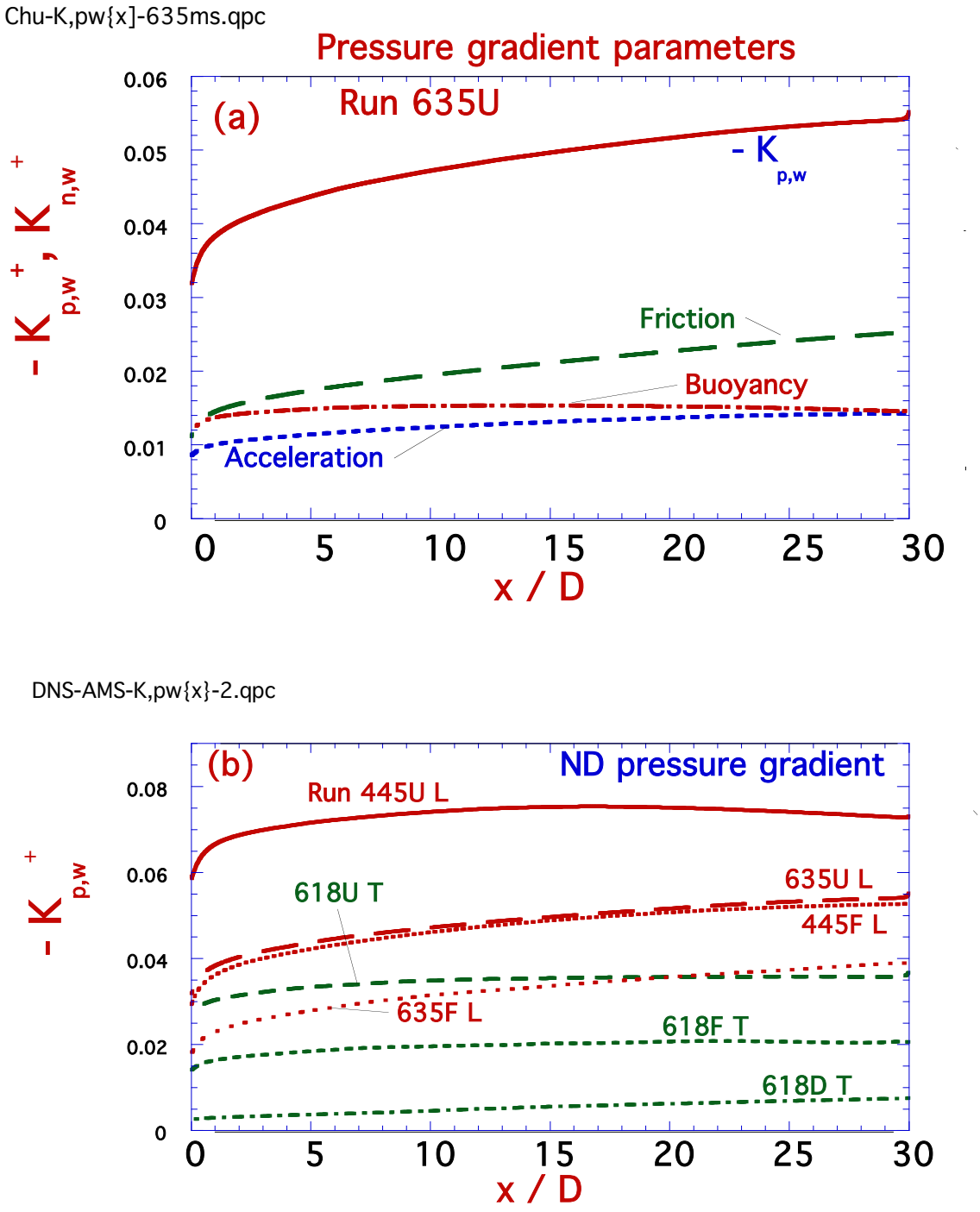

Fig. 8. Evolution of non-dimensional pressure gradients: (a) terms comprising ($-K_{p,w}^{+}$) plus total for Run 635U and (b) ($-K_{p,w}^{+}$) for cases of Table 2.

Since the convective thermal resistance is dominated by the molecular conduction layer near the wall, we have been evaluating K_p^+ with properties at wall temperature rather than bulk temperature. Some thoughtful engineers might wonder whether using bulk properties will give a better criterion for predicting the flow regime. From their definitions, one may show that $K_{p,b}^+ = K_{p,w}^+/[(\mu_w/\mu_b)\,(\rho_b/\rho_w)^{1/2}]$. If one applies the perfect gas approximation and a power law approximation for viscosity, $\mu \sim T^a$, this relation can be written as $K_{p,b}^+ \approx K_{p,w}^+/(T_w/T_b)^{a+(1/2)}$. Therefore, $|K_{p,b}^+| < |K_{p,w}^+|$ for a heated gas flow. A plot of the streamwise variation of $(-K_{p,b}^+)$ resembles Figure 8b but with smaller magnitudes (not shown). Again most of the laminarizing cases have high values and the turbulent runs have lower values. But laminarizing Runs 635U and 445F and turbulent Run 618U all have approximately the same magnitude for $K_{p,b}^+$ (within ± 0.0015). Also turbulent Run 618U has a higher value than laminarizing Run 635F. So $K_{p,b}^+$ cannot discriminate in all cases either.

The observations of the vortex behavior in Figure 5 and the evolutions of turbulence quantities presented by Chu and Bae lead us to wonder whether the non-dimensional radius $((r_w u_{\tau,w}/\nu_w) = (y_c u_{\tau,w}/\nu_w) = Re_{\tau,w})$ might provide a basis for a reasonable laminarization criterion. Figure 9 shows that this parameter ***does*** discriminate between turbulent and laminariing predictions for this set of DNS cases. Chu's and Bae's plots of TKE, Reynolds shear stresses and production of TKE give evidence of Run 635U laminarizing (in terms of fluctuating quantities) by (x/D) = 14 where $y_{c,w}^+$ has decreased to about 95. Figure 4 shows the bulges ("low-speed streaks") to be less vigorous at 15D and 25D than for Run 618U. For Run 445U the profiles of Chu and Bae indicate that the flow is laminarizing by (x/D) ≈ 3 and the flow visualization concurs; $y_{c,w}^+$ is less than ninety by this location. On the other hand, the profiles and flow visualizatoin for Run 618U at (x/D) ≈ 25 agree with our earlier conclusion that this case remains turbulent to the end of the computational domain where $y_{c,w}^+$ is about 115.

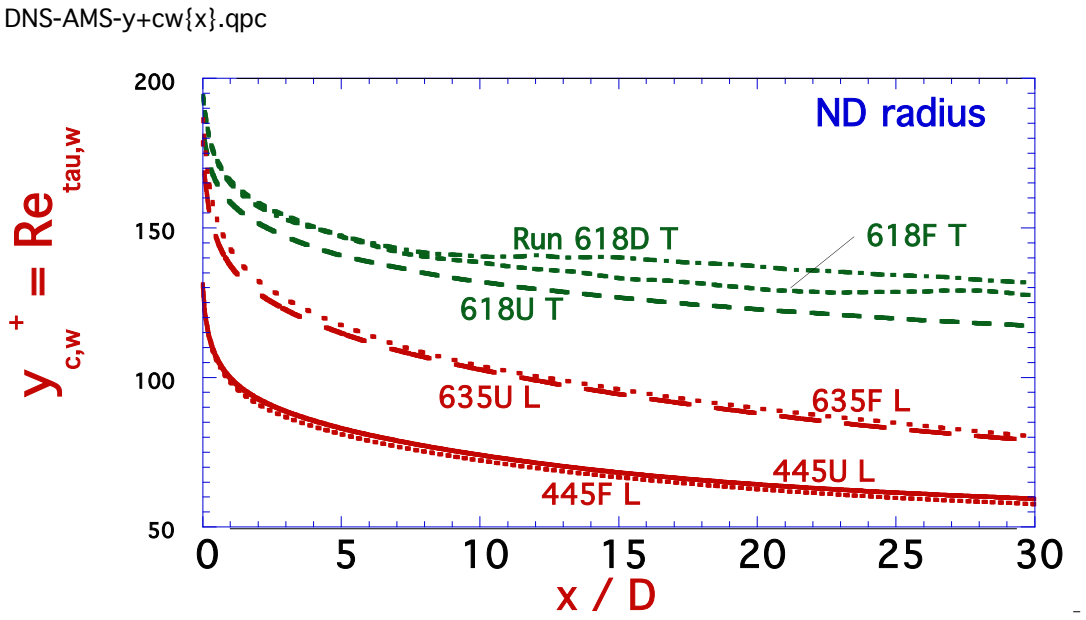

Fig. 9. Evolution of non-dimensional radii for DNS cases of Table 2.

These results indicate that the non-dimensional radius $y_{c,w}^+$ may be used as a criterion for laminarization with a value someplace in the range between 95 and 115. It would be desirable to develop DNS predictions for cases intermediate between our Runs 618 and Runs 635 as well as for longer domains (e.g., what happens to Run 618 further downstream?). As noted at the beginning of this section, for fully-developed flow with constant properties the shear-stress-gradient parameter of Patel and Head [JFM 1968] is the reciprocal of y_c^+; their chosen value is equivalent to a value of $y_{c,w}^+ < \sim 111$ as a criterion for laminarization.

A practical difficulty with using $y_{c,w}^+$ as a laminarization criterion is that it depends on knowing the skin friction coefficient in the developing flow with significant gas property variation. This quantity is usually a dependent variable not known to the analyst in advance. A possible alternate approach may be developed if we note that, for fully-developed flow with constant properties, $y_c^+ = Re_\tau = (Re_D/2)\,(f\{Re_D\}/2)^{-1/2}$ via their definitions. So a logical question becomes ---- can a Reynolds number serve as a useful laminarization criterion? We choose to check the modified wall Reynolds number to be consistent with our use of wall

properties. Figure 10 demonstrates that for this set of DNS predictions $Re_{w,m}$ provides a reasonable criterion for laminarization. From the same reasoning as for $y_{c,w}^+$ we conclude that a value between 2100 and 3000 would serve as a laminarization criterion for these DNS predictions (in the limit of low heating rates a good guess is about 2300). Again further DNS calculations would be desirable to reduce this range.

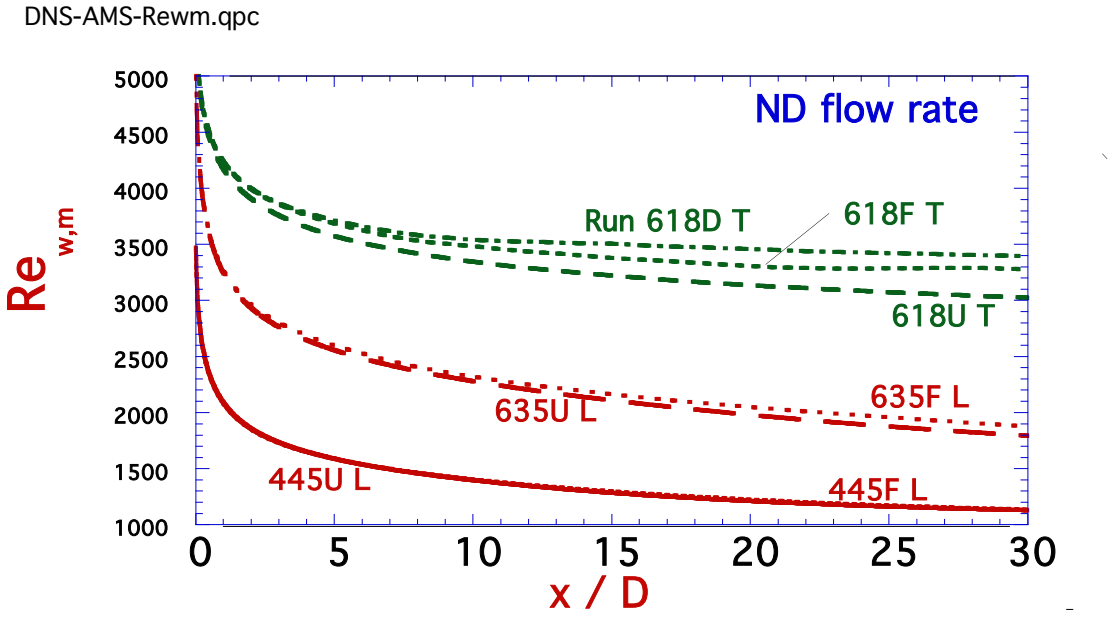

Fig. 10. Evolution of non-dimensional gas flow rate, $Re_{w,m} = (V_b D/\nu_w) = 4m/(\Pi D \rho_b \nu_w)$, for DNS cases of Table 2.

An operational advantage of using $Re_{w,m}$ as a criterion is that, for specified wall heat flux variations it can *approximately* be predicted via heat transfer correlations without need for the friction factor as for $y_{c,w}^+$. An energy balance yields the local bulk temperature, bulk fluid properties and $Re_b\{x\}$. For quasi-developed turbulent flow, the correlation of McEligot, Magee and Leppert [JHT 1965] with $(T_w/T_b)^{-1/2}$ then allows application of the binomial formula [p. 7, Burrington 1948] to deduce T_w/T_b directly without need for iteration [McEligot, p. 155, Adv.Trans.Proc. 1986]. (For a laminar prediction a correlation by Worsoe-Schmidt [IJHMT 1966] can be employed.) The modified wall Reynolds number, $Re_{w,m} = Re_b (\nu_b/\nu_w)$, is then calculated from Re_b and the properties at T_w and T_b to check the criterion.

5. Discussion

For low "turbulent" Reynolds numbers in strongly-heated vertical gas flow, fundamental results of DNS have been examined to deduce differences between cases which "revert" to turbulent and those that yield integral parameters which correspond to laminar flow (called laminarizing or laminarized). Key objectives are (1) to examine the streamwise evolution of near-wall flow structures and (2) to determine which, if any, proposed laminarization parameters could be used to discriminate between turbulent and laminarizing flows resulting.

The typical experiment is idealized as a step change to a uniform wall heat flux after a vertical turbulent flow is fully-developed. The DNS employed are by J. H. Bae [Bae et al. Phys.Fl. 2006] and Chu [Chu, Laurien and McEligot, IJHMT 2016] modeling the experiments of Shehata [IJHMT 1998]; the seven cases examined include upflow (U), downflow (D) and zero buoyancy (F), all with significant air property variation. Evaluation of the streamwise variation of popular acceleration and buoyancy parameters forecast that Run 618U would be expected to remain turbulent, Run 445U to laminarize and Run 635U to be uncertain. By comparison to the laminar thermal entry analysis of Worsoe-Schmidt [IJHMT 1966] and the downstream turbulent correlation of McEligot, Magee and Leppert [JHT 1965], cases were categorized as "turbulent" or "laminarizing." On this basis Runs 618U/F/D were labeled "turbulent" and Runs 635U/F and 445U/F were taken as "laminarizing" or "laminarized."

Since the convective heat transfer in these low-Reynolds-number flows is dominated by the convective thermal resistance in the immediate wall region, the ***evolution of near-wall fluid structures*** was studied via their instantaneous transverse cross-sections in the r-θ plane. **All** cross-sections showed evidence of a ring of irregular quasi-streamwise vortices near the wall. We hypothesize that this observed prevalence of the pattern implies that it is a fundamental flow structure, i.e., a preferred mechanism to accommodate the velocity difference between the turbulent central core and the no-slip wall. The existence of streamwise vortices in the near-wall region has been noted for decades. The transverse advection of this fundamental structure is hypothesized to provide a path of least resistance to the transport of streamwise momentum in

the wall-normal direction for the turbulent cases. Several previous investigators have provided evidence which supports this hypothesized model [Görtler, Göttingen 1940; Townsend, Camb.Soc. 1951; Görtler, Braunschweig 1955; Bakewell and Lumley, Phys.Fl. 1967; Blackwelder and Eckelmann, JFM 1979; Wood, thesis 1980; Smith and Schwartz, Phys.Fl. 1983; Bejan, text 1984: Kasagi, Hirata and Nishino, Exp.Fl. 1986; Bradshaw, Stewartson Lecture 1992; Brooke and Hanratty, Phys.Fl. 1993; Jimenez, Phys.Fl. 2013]. In general, the present observations of Chu's DNS results and the proposed model are consistent with Jimenez's description [Phys.Fl. 2013] but with slightly different emphases on the fluid structure.

The wall-normal heights of the well-developed vortices appeared to be about 50-60 wall units; the turbulent cases (Run 618U plus the entering flows of Runs 635U and 445U) had non-dimensional tube radii about twice as large as these vortices so that the turbulent core filled a quarter or more of the cross section. For fully-developed, unheated laminar flow, the centerline distance is $y_c^+ = (2\ Re_D)^{1/2}$ in wall coordinates. It is interesting to note that a typical value of a transition Re_D in common flows is about 2300, e.g., eqn. 15-1 by Schlichting and Gersten [text 2000], where $y_c^+ \approx 68$ for fully-developed laminar flow. So at this Reynolds number there should be room enough for the flow pattern to shift to significant streamwise vortices, giving lower resistance to transverse momentum transfer and a version of turbulent flow (in the sense of the Reynolds decomposition). If the mass flow rate is maintained so Re_D remains at 2300, the non-dimensional radius of the apparent "turbulent" flow could become $y_c^+ \approx 0.0994\ Re^{7/8} \approx 87$ (using the turbulent Blasius correlation [Berlin 1913]). This size should easily accommodate the pattern of streamwise vortices and the flow could be expected to remain turbulent.

The sustaining driving force for the vortex flow pattern comes from the momentum of the turbulent core flow induced by the streamwise pressure gradient required to maintain the desired flow rate. Otherwise, at the low Reynolds numbers of interest here, the core flow has a relatively minor role. The streamwise velocity in the core is near uniform so the exchange of fluid packets there does not provide large momentum transfer; it is essentially "well-mixed." In the denominator of $R' = [(\partial U/\partial y)/\tau\{y\}] = 1/(\mu + \mu_{turb})$, μ_{turb} can be approximated as $\kappa\ u_\tau\ \rho\ y$. With heating from the wall the gas is denser in the core than at the wall and y increases there so

R' is reduced. At these low Reynolds numbers, the thermal resistance of the turbulent core flow tends to be negligible. If we define the thermal resistance from the relation q_w" $R_{th} = (T_w - T_b)$, we find that most of R_{th} occurs in a small region near the wall (e.g., see Figure 1 by McEligot et al. [6ISCO2PCS 2018]).

Kasagi, Hirata and Nishino [Exp.Fl. 1986] credit Bakewell and Lumley [Phys.Fl. 1967], Lee, Eckelman and Hanratty [JFM 1974] and others with suggesting that streamwise vortices are the primary turbulence mechanism for the production of Reynolds stress and turbulence energy in the near-wall region. For DNS problems with axi-symmetric boundary conditions, like the present study, mean quantities are typically determined by forming a circumferential space-average and then a temporal average. For turbulent and transitional flows, the Reynolds decomposition is applied to deduce "turbulent" quantities as the differences from such mean results. While turbulence may be described as a three-dimensional motion that is time-dependent [Bradshaw text, 1971], a steady two-dimensional laminar flow --- such as a long streamwise vortex --- will provide apparent mean Reynolds shear stresses $<-\rho uv>$ via such calculations. Often $<uv>$ is called a "turbulent" shear stress and may be employed to calculate a turbulent viscosity or eddy diffusivity for momentum.

If we consider the prevalent near-wall vortices to be long in the streamwise direction and to persist for a considerable fraction of time, their effects may be approximated by a two-dimensional ***steady*** vortex model. Kasagi, Hirata and Nishino [Exp.Fl. 1986] approximated a temporal vortex motion with spatial and temporal sinusoidal functions and called it a Simple Pseudo-Vortical Motion model. To demonstrate how a field of **steady** streamwise vortices near the wall could provide apparent turbulent statistics, we can select a single instant from their flow field (their equations 12-14) and treat the vortex as steady. Figure 11 provides resulting distributions of the wall-normal velocity, the total streamwise velocity ($u_{total}^+\{y^+, z^+\} = U^+\{y^+\} + u^+\{y^+, z^+\}$), and the pointwise non-dimensional "Reynolds shear stress" near the wall. (In the nomenclature of Kasagi, Hirata and Nishino we chose the instant $t^+/T^+ = 0.536$ and phase $\varphi = +3/16$ and accepted their values for other parameters.) The vortex approximated

has a width Δz^+ of fifty centered on $z^+ = 0$, corresponding to a wave length λ^+ of 100 between low speed streaks. Typical streamlines in the y-z plane are shown in their Figure 16.

In Figure 11a we see the circulating vortex has a wall-normal outflow, $v^+ > 0$, on the left, carrying fluid with lower streamwise velocity from the near-wall region and thereby forming an apparent "low speed streak" in Figure 11b and producing some apparent "turbulent" kinetic energy (not shown) and the apparent pointwise Reynolds shear stress in Figure 11c (note the negative sign on the ordinate) near the edge of the vortex model. On the right the circulation of the vortex produces a wallward flow from the outer layer, creating a "high speed streak" or a result of Bradshaw's "splat" [Wood thesis, 1980; Lecture 1992] and producing Reynolds shear stress.

SSPVM--0.536-(v+).qpc

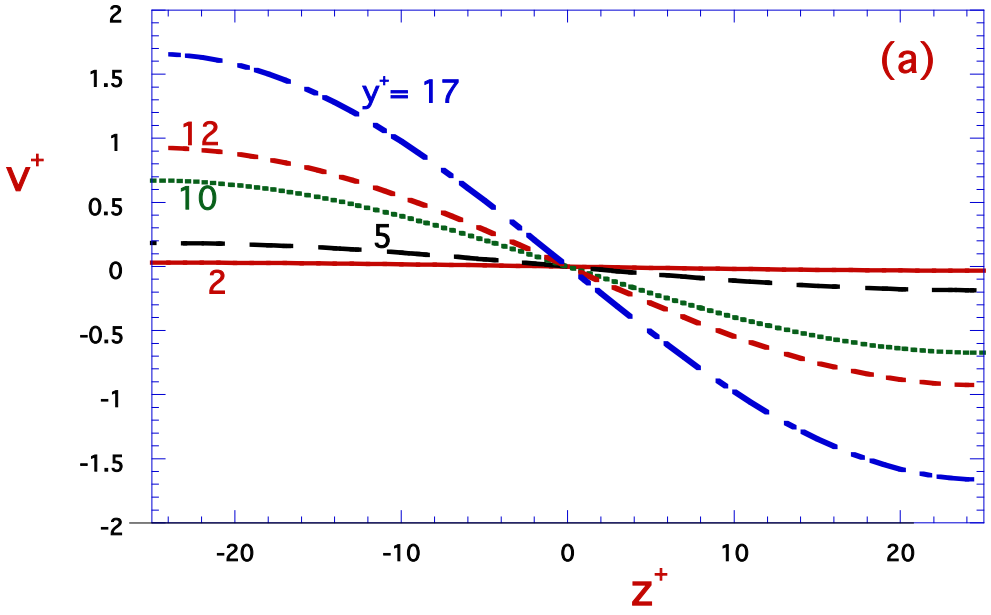

SSPVM--0.536-u{z}.qpc

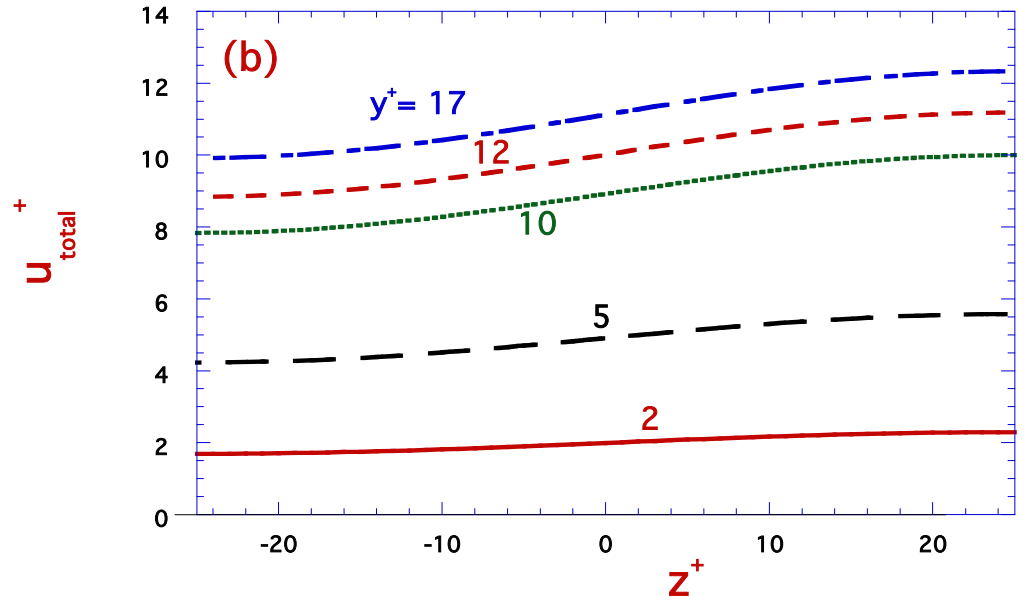

SSPVM--0.536-(-uv).qpc

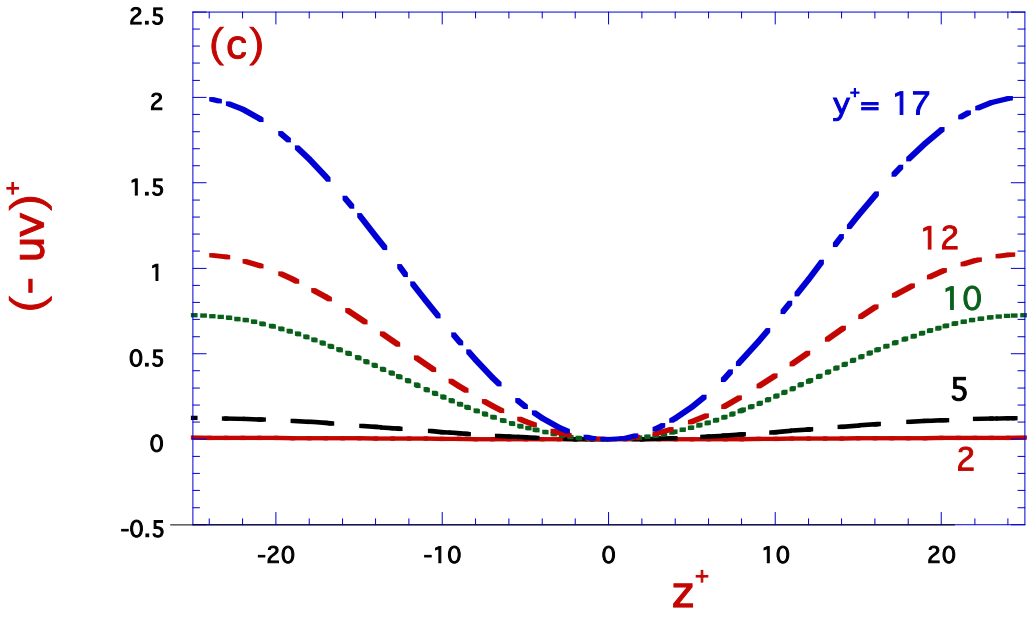

Fig. 11. Spanwise distributions from present "Simpler Steady Pseudo-Vortical Motion" model in wall coordinates: (a) wall-normal component, (b) total streamwise velocity component and (c) "Reynolds shear stress."

We averaged (-uv{z^+}) with respect to z to form a "mean Reynolds shear stress" and then considered a high Reynolds number flow, to justify a constant shear layer approximation, and integrated with respect to y to predict $U^+\{y^+\}$ for this near-wall region. The result is compared to the DNS prediction of Schlatter et al. [Phys.Fl. 2009] at $Re_\theta = 2400$ in Figure 12a. For this near-wall region, this simple steady pseudo-vortex motion would provide a reasonable approximation of this statistic of the fully-turbulent DNS calculation. *That is, a simple steady streamwise vortex can provide the key mean statistics of the viscous layer without needing additional random motions to simulate turbulence*. (The model of Kasagi, Hirata and Nishino has several parameters which might be modified to obtain better agreement and/or representation of different sized vortices.) Jimenez [Phys.Fl. 2013] also observes that steady or quasi-steady solutions can approximate the flow statistics well. A possible implication of this last observation is that transient features (such as "bursts") are not important, have self-cancelling contributions to the statistics and/or are relatively passive events.

The resistance to wall-normal transport of x-directed momentum can be defined via the relationship $\tau\{y\} = (1/R')\ \partial U/\partial y$ where R' is the resistance per unit distance (depth). In the present example with the constant shear layer idealization, this definition can be written as $R^+ = \mu R' \approx \partial U^+/\partial y^+$. Figure 12b compares $R^+\{y^+\}$ for laminar flow to the predictions of the SSPVM model and Schlatter et al. in the near-wall region; one sees a steady vortex can provide a path of significantly less resistance (for x-momentum transported in the wall-normal direction) than pure molecular shear as in the one-dimensional laminar case, as suggested in the earlier discussion.

In a paper examining the conditions under which a universal relationship between the turbulent shear stress and the streamwise mean velocity could exist close to the wall, Townsend [JFM 1961] devoted the last paragraph to introducing the idea of there being two components of turbulent motion near the wall: active and inactive. The active component would be determined by the turbulent shear stress distribution and be responsible for the turbulent transfer and the inactive component would not transfer momentum. Since the predicted Reynolds shear stress distribution of the SSPVM model provides a near-wall streamwise velocity distribution of the same magnitude as the DNS, one might conclude that such a flow could correspond to

Townsend's "active motion" in this region. His "inactive motion" would then contribute to an increase in the TKE components and possibly a randomizing of the vortex position and instantaneous details.

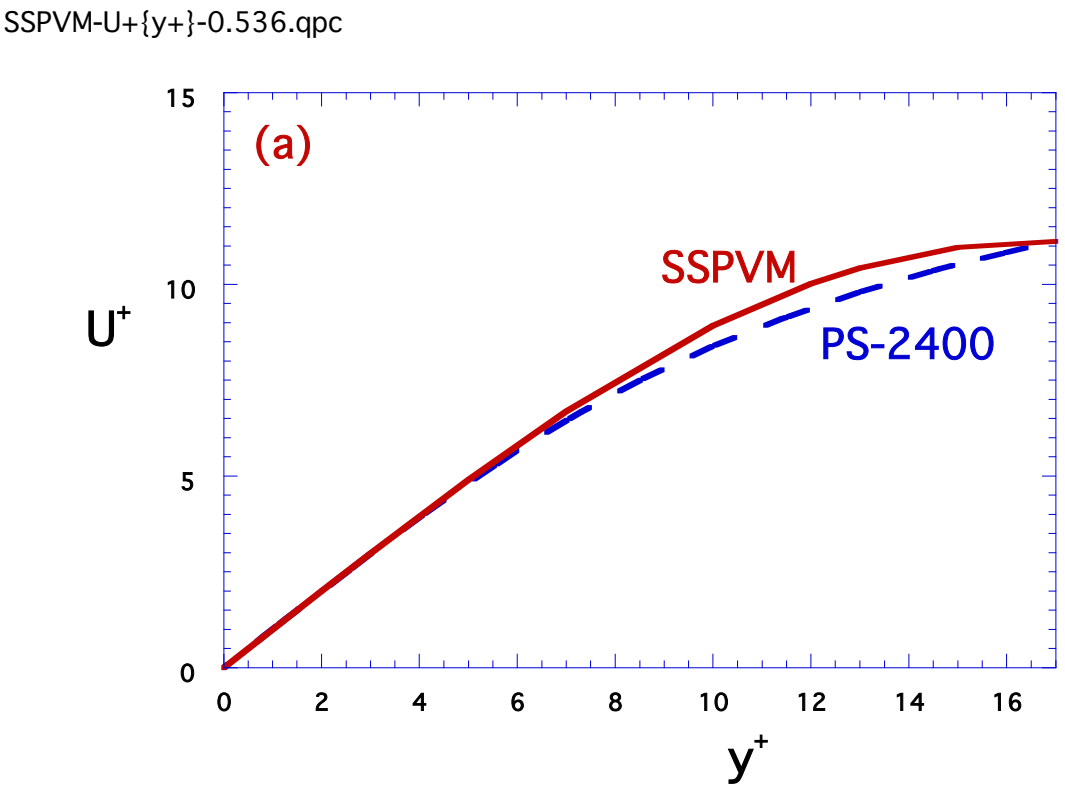

Fig. 12a. Near-wall predictions of mean streamwise velocity component for high Reynolds numbers by present "Simpler Steady Pseudo-Vortical Motion" model (solid curve) and by direct numerical simulation of Schlatter et al. [Phys.Fl. 2009] at $Re_\theta = 2400$ (dashed curve).

As noted, our hypothesis --- that near-wall streamwise vortices provide a fundamental flow structure --- is supported by the limited present observations and by those in the related literature cited. That is, they appear to provide a key mechanism for accommodating the velocity difference between the turbulent core and the no-slip wall. The qualitative ideas discussed are supported by the existing related quantitative literature mentioned above concerning the behavior of the structure in near-wall turbulent flows. The results from the SSPVM model provide

additional support to our hypothesis that near-wall quasi-streamwise vortices serve as a fundamental flow structure to act as a mechanism for accommodating the velocity difference between the turbulent core and the no-slip wall. These results demonstrate that these vortices can yield the characteristic mean velocity distribution connecting the "linear" (molecular shear) layer to the "logarithmic layer" in wall-bound turbulent shear flows. And, in turn, for two-layer turbulence models [Prandtl, Phys.Z. 1910; Laurien, NERS 2016] this distribution can establish the coordinates of the intersection giving the viscous layer thickness, y_V^+.

SSPVM-R+{y+}-0.536.qpc

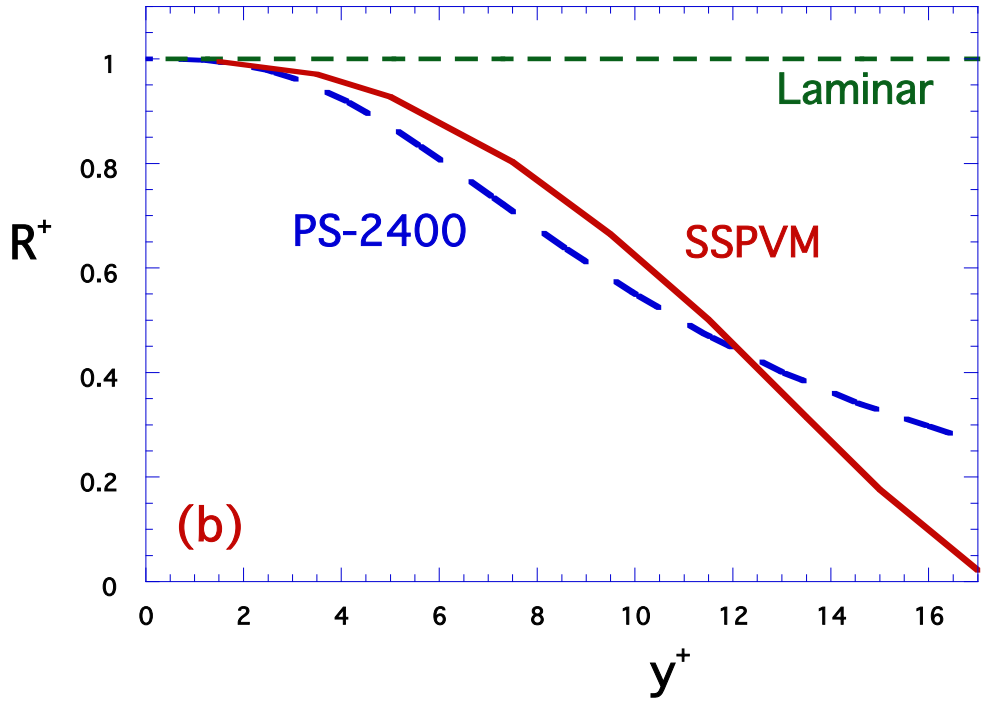

Fig. 12b. Comparison of non-dimensional resistance (to transport of x-momentum in the wall-normal direction) predicted by the "SSPVM" model (solid curve) to that of a pure molecular shear flow (labeled "laminar") and DNS predictions by Schlatter et al. [Phy.Fl. 2009] at Re_θ = 2400 (dashed curve).

The apparent laminarization of Runs 635U and 445U corresponds to their non-dimensional tube radii becoming less than about twice the height of energetic streamwise

vortices. The cross sections of the laminarizing runs (635U and 445U) show the physical widths of the vortices to grow in the downstream flow. As the flow progresses downstream the aspect ratio of the circulating vortex flow appears to change so a larger proportion of its flow path would be shear flow along the wall, providing relatively more resistance to the circulation driving the vortex flow to and from the wall so that momentum advection is reduced. The heating assists as well; increasing q^+ increases the wall temperature and, therefore, the kinematic viscosity in the wall region so the molecular layer grows more rapidly. Vortex flow from the wall (our "bulges," others "low-velocity streaks") becomes less vigorous so its contribution to reduction of resistance to transverse u-momentum transfer gradually becomes negligible. This effect is demonstrated quantitatively by the reduction (and for Runs 445U/F near disappearance) of the circumferentially-averaged wall-normal transport of streamwise momentum transfer (aka Reynolds shear stress) in Figures 10b, 10c and 10d by Chu.

In order to treat ***cases where two laminarizing phenomena*** --- acceleration and buoyancy --- ***are both likely to be significant***, the streamwise momentum equation containing both was rearranged to evaluate a non-dimensional pressure gradient. In wall coordinates this parameter is the same as recommended by Bankston (our $-K_{p,w}^+$) primarily for cases where acceleration was believed to be the dominant cause (small tubes). From their definitions, relations to the popular K_V and $Bo_{J,b}$* were derived.

The ***evolutions of several proposed laminarization parameters*** were evaluated for the seven DNS cases to examine whether the values of any could serve as a criterion for the apparent flow regime which resulted. For the most part, we chose parameters with gas properties based on the wall temperature. The values of two pressure gradient parameters --- ($-K_{p,w}^+$) of Bankston [JHT 1970] and our interpretation of $\Lambda_i\{x\}$ of Narasimha and Sreenivasan [Adv.Appl.Mech. 1979] --- were only partially successful at discriminating between remaining laminar and reverting to turbulent. For the present cases, both had a range of values where either laminar or turbulent flow might occur, i.e., they did not discriminate (Figures 7b and 8b).

Two possible criteria did discriminate between the present cases: they employed the non-dimensional radius ($y_{c,w}^+ = Re_{\tau,w}$) and the modified wall Reynolds number ($Re_{w,m}$). However, in both cases the magnitude of the criterion is a bit more uncertain than desirable. The quantity $y_{c,w}^+$ can be considered to be related to the shear-stress-gradient parameter of Patel and Head [JFM 1968] and the present results indicate that $Nu_b\{x\}$ will agree with a downstream turbulent correlation when $y_{c,w}^+$ exceeds a value that is between 95 and 115. These magnitudes correspond to the radius becoming about twice the height of the near-wall vortex ring or more. For $Re_{w,m}$ the range in which the laminarization criterion would fall is 2100 to 3000. As noted earlier, $Re_{w,m}$ would be easier to use operationally because it only requires a heat transfer prediction and not a skin friction prediction as well. Thus, for applications like the Shehata experiment, thermal engineers may use a variable-property turbulent heat transfer correlation or CFD with a successful variable-property turbulence model such as that of Ezato [JHT 1999] when $Re_{w,m} > 3000$ or $y_{c,w}^+ > 115$. Likewise, for $Re_{w,m} < 2100$ or $y_{c,w}^+ < 95$, a variable-property laminar entry correlation (e.g., Worsoe-Schmidt [IJHMT 1966]) or variable-property laminar thermal fluid dynamics code [Worsoe-Schmidt and Leppert, IJHMT 1965; Bankston and McEligot, IJHMT 1970] should be adequate. For ranges in between, we can only recommend evaluating both and selecting the worst case for the situation. So it would be desirable to have further DNS predictions with non-dimensional heat fluxes for $0.0018 < q^+ < 0.0035$ to narrow the ranges for the criteria.

The "short" DNS cases in this study represent a version of apparent laminarization dependent on evolution of the thermal entry boundary layer. All runs begin with the thermal boundary layer within the existing molecular transport layer (i.e., effectively laminar). This initial molecular transport layer thickness is determined by the entering Reynolds number. In terms of mean quantities, the so-called laminarization in the cases treated here is a situation where the laminar entry thermal boundary layer remains within the molecular conduction sublayer as described in our earlier paper [McEligot et al., IJHMT 2018]; Runs 635U/F and 445U/F are examples. Runs 618U/F/D apparently revert to turbulent when their thermal entry boundary layer grows to the turbulent core region, where there is apparent turbulent transport,

beyond their molecular momentum transport sublayer (which is also growing slightly as the Reynolds number decreases).

Another version of laminarization would be of interest further downstream after the thermal field becomes quasi-developed, e.g., for Run 618U beyond the domain of the present DNS. With the heating continuing, the local Reynolds number will continue to decrease and one expects a situation will occur where the integral heat transfer parameters decrease below their turbulent predictions or "deteriorate." Bankston [JHT 1970] demonstrates some likely examples in his Figure 9a. Situations with heat flux increasing in the streamwise direction, as in a nuclear reactor, may also encounter this behavior. Thus, it would also be desirable to have further DNS calculations for longer domains over ranges of flow rates, heating rates, buoyancy values and axially varying heat flux distributions.

Acknowledgements

We thank Prof. J.-i. Lee of KAIST for providing his tabulated data and his continued friendly help over the years. This study was partly supported by the Korea/U.S. International NERI (Nuclear Energy Research Initiative) program under the auspices of the Korea Institute of Science and Technology Evaluation and Planning (KISTEP) and also by the Creative Research Initiative (CRI) program of KISTEP, by the Forschungsinstitut für Kernenergie und Energiewandlung, by the Ministerium für Wissenschaft, Forschung und Kunst Baden-Württemberg, by the U. S. DoE Office of Nuclear Energy's Nuclear Energy University Program (NEUP) contract DE-NE0008412 and by the Center for Advanced Energy Studies via U. S. Department of Energy Idaho Operations Office Contract DE-AC07-05ID14517. Accordingly, the U.S. Government and its representatives retain a nonexclusive, royalty-free license to publish or reproduce the published form of this contribution, or allow others to do so, for U.S. Government purposes.

References cited

Arani, B. O., C. E. Frouzakis, J. Mantzaras, F. Lucci and K. Boulouchos, 2018. Direct numerical simulation of turbulent channel-flow catalytic combustion: Effects of Reynolds number and catalytic reactivity. *Combustion and Flame*, 187, pp. 52-66.

Bae, J. H., J. Y. Yoo, H. Choi and D. M. McEligot, 2006. Effects of large density variation in strongly-heated internal air flows. *Phys. Fluids*, 18, pp. 075102-1 to -25.

Bae, J. H., J. Y. Yoo, H. Choi and D. M. McEligot, 2008. Structure of turbulent boundary layers developing in a heated vertical annular pipe at supercritical pressure. *Phys. Fluids*, 20, pp. 055108-1 to - 20 . Available online as doi:10.1063/1.2927488.

Bakewell, H. P., and J. L. Lumley, 1967. Viscous sublayer and adjacent wall region in turbulent pipe flow. *Phys. Fluids*, 10, pp. 1880-1889.

Bankston, C. A., 1970. The transition from turbulent to laminar gas flow in a heated pipe. *J. Heat Transfer,* 92, pp. 569-579.

Bankston, C. A., and D. M. McEligot, 1970. Turbulent and laminar heat transfer to gases with varying properties in the entry region of circular ducts. *Int. J. Heat Mass Transfer*, 13, pp. 319-344.

Bejan, A., 1984. *Convection heat transfer*. New York: John Wiley and Sons.

Blackwelder, R. F., 1988. Coherent structures associated with turbulent transport. *Trans. Phen. Turb. Flows* (Ed.: M. Hirata and N. Kasagi), pp. 69-88, New York: Hemisphere.

Blackwelder, R. F., and H. Eckelmann, 1979. Streamwise vortices associated with the bursting phenomenon. *J. Fluid Mech.*, 94, pp. 577-594.

Blackwelder, R. F., and L. S. G. Kovasznay, 1972. Large scale motion of a turbulent boundary layer during relaminarization. *J. Fluid Mech.*, 53, pp. 61-83.

Blasius, H., 1913. Das Ähnlichkeitsgesetz bei Reibungsvorgängen in Flüssigkeiten. *Forsch. Arb. Ing. Wes.*, No. 131, pp. 1-40, Berlin.

Bradshaw, P., 1971. *An introduction to turbulence and its measurement*. Oxford: Pergamon.

Bradshaw, P., 1992. Turbulence: The chief outstanding difficulty of our subject. Stewartson Memorial Lecture. Available via ntrs.nasa.gov/archive/nasa/casi.ntrs.nasa.gov/19930018239.pdf.

Bradshaw, P., and Y. M. Koh, 1981. A note on Poisson's equation for pressure in a turbulent flow. *Phys. Fluids*, 24, p. 777.

Brooke, J. W., and T. J. Hanratty, 1993. Origin of turbulence-producing eddies in a channel flow. *Phys. Fluids A*, 5 (4), pp. 1011-1022.

Burington, R. S., 1948. *Handbook of mathematical tables and formulas, 3rd ed*. Sandusky, Ohio: Handbook Publishers, Inc.

Cantwell, B. J., 1981. Organized motion in turbulent flow. *Ann. Rev. Fluid Mech*, 13, pp. 437-515.

Chu, X., W. Chang, S. Pandey, J. Luo, B. Weigand and E. Laurien, 2018. A computationally light data-driven approach for heat transfer and hydraulic characteristics modeling of supercritical fluids. From DNS to DNN. *Int. J. Heat Mass Transfer*, 123, pp. 629-636.

Chu, X., E. Laurien and D. M. McEligot, 2016. Direct numerical simulation of strongly heated air flow in a vertical pipe. *Int. J. Heat Mass Transfer*, 101, pp. 1163-1176.

Corino, E. R., and R. S. Brodkey, 1969. A visual observation of the wall region in turbulent flow. *J. Fluid Mech.*, 37, pp. 1-30.

Dittus, F. W., and L. M. K. Bölter, 1930. Heat transfer in automobile radiators of the tubular type. *Publications in Eng.*, U. California, 2, pp. 443-461.

Drexel, R. E., and W. H. McAdams, 1945. Heat-transfer coefficients for air flowing in round tubes, rectangular ducts and around finned cylinders. NACA Wartime Report 108, February.

Eggels. J. G. M., F. Unger, M. H. Weiss, J. Westerweel, R. J. Adrian, R. Friedrich and F. T. M. Nieuwstadt, 1994. Fully developed turbulent pipe flow: a comparison between direct numerical simulation and experiments. *J. Fluid Mech.*, 268, pp. 175-210.

Ezato, K., A. M. Shehata, T. Kunugi and D. M. McEligot, 1999. Numerical predictions of transitional features of turbulent gas flows in circular tubes with strong heating. *J. Heat Transfer,* 121, pp. 546-555.

Gnielinski, V., 1976. New equations for heat and mass transfer in turbulent pipe and channel flow. *Int. Chem. Engr.*, 16, pp. 359-368.

Görtler, H., 1940. Über eine dreidimensionale Instabilität laminarer Grenzschichten an konkaven Wänden. Nachr. Wiss. Ges. Göttingen, Math. Phys. Klasse, Neue Folge 2, No. 1.

Görtler, H., 1955. Dreidimensionale Instabilität der ebenen Staupunktströmung gegenüber wirbelartigen Störungen. *Fifty Years of Boundary Layer Research* (Ed.: W. Tollmien and H. Görtler), Braunschweig, pp. 303-314.

He, S., K. He and M. Seddighi, 2016. Laminarisation of flow at low Reynolds number due to streamwise body force. *J. Fluid Mech.*, 809, pp. 31-71.

Jackson, J. D., M. A. Cotton and B. P. Axcell, 1989. Studies of mixed convection in vertical tubes. *Int. J. Heat Fluid Flow*, 10, pp. 2-15.

Jimenez, J., 2013. Near-wall turbulence. *Phys. Fluids*, 25, pp. 101302-1 to -28.

Jimenez, J., 2018. Coherent structures in wall-bounded turbulence. *J. Fluid Mech.*, 842, pp. P1-1 to -100.

Kays, W. M., 1966. *Convective heat and mass transfer*. New York: McGraw-Hill.

Kasagi, N., M. Hirata and K. Nishino, 1986. Streamwise pseudo-vortical structures and associated vorticity in the near-wall region of a wall-bounded turbulent shear flow. *Exp. Fluids*, 4, pp. 309-318.

Kline, S. J., W. C. Reynolds, F. A. Schraub and P. W. Rundstadler, 1967. The structure of turbulent boundary layers. *J. Fluid Mech.*, 30, pp. 741-773.

Kovasznay, L. S. G., 1970. The turbulent boundary layer. *Ann. Rev. Fluid Mech*, 2, pp. 95-112.

Launder, B. E., 1964. Laminarization of the turbulent boundary layer by acceleration. MIT Gas Turbine Lab. Rpt. 77. Also NASA N66-16042.

Laurien, E., 2016. Implicit equation for hydraulic resistance and heat transfer including wall roughness. *J. Nuc. Engr. Rad. Sci.*, 2, pp. 021016-1 to -6.

Lee, J.-i., 2007. Gas heat transfer in a heated vertical channel under deteriorated turbulent heat transfer regime. Ph.D. thesis, M. I. T., April.

Lee, J.-i, P. Hejzlar, P. Saha, M. S. Kazimi and D. M. McEligot, 2008. Deteriorated turbulent heat transfer (DTHT) of gas up-flow in a circular tube: Experimental data. *Int. J. Heat Mass Transfer*, 51, pp. 3259-3266.

Lee, J.-i., P. Hejzlar, P. Saha, M. S. Kazimi and D. M. McEligot, 2008. Deteriorated turbulent heat transfer of gas up-flow in a circular tube: Heat transfer correlations. *Int. J. Heat Mass Transfer*, 51, pp. 5318-5326.

Lee, M. K., L. D. Eckelman and T. J. Hanratty, 1974. Identification of turbulent wall eddies through the phase relation of the components of the fluctuating velocity gradient. *J. Fluid Mech.*, 66, pp. 17-33.

Lee, M., and R. D. Moser, 2015. Direct numerical simulation of turbulent channel flow up to $Re_\tau \approx 5200$. *J. Fluid Mech.*, 774, pp. 395-415.

Leveque, A., 1928. Les lois de la transmission de chaleaur par convection. *Ann. Mines Mem. Ser.,* 12-13, pp. 201-299, 305-362 and 381-415.

Li, J. K. 1994. Studies of buoyancy-influenced convective heat transfer to air in a vertical tube. Ph.D. thesis, U. Manchester.

Liepmann, H. W., 1943. Investigations on laminar boundary-layer stability and transition on curved boundaries. NACA Wartime Report W-107, ACR No. 3H30.

Liepmann, H. W., 1945. Investigation of boundary layer transition on concave walls. NACA Wartime Report ACR No. 4J28.

Mack, L. M., 1979. Effects due to heat transfer and compressibility. *Boundary layer theory, 7th ed*. (Main author: H. Schlichting), Section XVIIe, pp. 514-525, New York: McGraw-Hill.

Marusic, I., and J. P. Monty, 2019. Attached eddy model of wall turbulence. *Ann. Rev. Fluid Mech*, 51, pp. 49-74.

McEligot, D. M., 1963. Effect of large temperature gradients on turbulent flow of gases in the downstream region of tubes. TID-19446, Office of Technical Services, Washington, D. C.: U. S. Department of Commerce.

McEligot, D. M., 1986. Convective heat transfer in internal gas flows with temperature-dependent properties. *Adv. Transport Processes,* 4, pp. 113-200.

McEligot, D. M., X. Chu, R. S. Skifton and E. Laurien, 2018. Internal convective heat transfer to gases in the low-Reynolds-number "turbulent" range. *Int. J. Heat Mass Transfer,* 121, pp. 1118-1124.

McEligot, D. M., C. W. Coon and H. C. Perkins, 1970. Relaminarization in tubes. *Int. J. Heat Mass Transfer*, 13, pp. 431-433.

McEligot, D. M., and H. Eckelmann, 2006. Laterally converging duct flows: Part 3. Mean turbulence structure in the viscous layer. *J. Fluid Mech*., 549, pp. 25-59.

McEligot, D. M., and J. D. Jackson, 2004. "Deterioration" criteria for convective heat transfer in gas flow through non-circular ducts. *Nuc. Engr. Design,* 232, pp. 327-333.

McEligot, D. M., E. Laurien, W. Wang and S. He, 2018. The dominant thermal resistance approach for heat transfer to supercritical fluids. Paper No. 32, Proc., 6th Int. Supercritical CO_2 Power Cyc. Symp., Pittsburgh, 27-29 March. http://sco2symposium.com/www2/sco2/papers2018.htm.

McEligot, D. M., P. M. Magee and G. Leppert, 1965. Effect of large temperature gradients on convective heat transfer: The downstream region. *J. Heat Transfer,* 87, pp. 67-76.

Moretti, P. M., and W. M. Kays, 1965. Heat transfer in a turbulent boundary layer with varying free-stream velocity and varying surface temperature -- an experimental study. *Int. J. Heat Mass Transfer*, 8, pp. 1187-1202.

Murphy, H. D., F. W. Chambers and D. M. McEligot, 1983. Laterally converging flow. I: Mean flow. *J. Fluid Mech.*, 127, pp. 379-401.

Nachtsheim, P. R., 1963. Stability of the free convection boundary layer flow. NASA TN D-2089.

Narasimha, R., and K. R. Sreenivasan, 1979. Relaminarization of fluid flows. *Adv. Appl. Mech.,* 19, pp. 221-309.

Nemati, H., A. Patel, B. J. Boersma and F. Pecnik, 2016. The effect of thermal boundary conditions on forced convection heat transfer to fluids at supercritical pressure. *J. Fluid Mech.*, 800, pp. 531-556.

Pandey, S., X. Chu and E. Laurien, 2017. Investigation of in-tube cooling of carbon dioxide at supercritical pressure by means of direct numerical simulation. *Int. J. Heat Mass Transfer*, 114, pp. 944-957.

Patel, V. C., and M. R. Head, 1968. Reversion of turbulent to laminar flow. *J. Fluid Mech.*, 34, pp. 371-392.

Perkins, K.R., 1975. Turbulence structure in gas flows laminarizing by heating. Ph.D. thesis. University of Arizona.

Prandtl, L., 1910. Eine Beziehung zwischen Wärmeaustausch und Strömungswiderstand der Flüssigkeit. *Physik. Z.,* 11, pp.1072-1078.

Reynolds, H. C., 1968. Internal low Reynolds number turbulent heat transfer. Ph.D. thesis. University of Arizona. DDC AD-669 254.

Robinson, S. K., 1991. Coherent motions in the turbulent boundary layer. *Ann. Rev. Fluid Mech*, 23, pp. 601-639.

Rotta, J. C., 1962. Turbulent boundary layers in incompressible flow. *Progress in Aeronautical Sciences,* Vol. 2, pp. 1-219, Oxford: Pergamon Press.

Rudra, A., S. Banerjee, M. Kawaji, A. Obabko and S. Patel, 2018. Sustaining turbulence in a very long pipe towards studying heat driven turbulent gas relaminarization. Proc., Adv. Thermal Hydraulics, Amer. Nuc, Soc. Winter Meeting, Orlando, 11-15 November.

Satake, S., H. Sawamura, M. Kimura and T. Kunugi, 2015. DNS of turbulent heat transfer in pipe flow via the HELIOS supercomputer system at IFERC-CSC. *Fusion Sci. Tech.,* 68, pp. 640-643.

Schlatter, P., R. Örlü, Q. Li, G. Brethouwer, J. H. M. Fransson, A. V. Johansson, P. H. Alfredsson and D. S. Henningson, 2009. Turbulent boundary layers up to Re_τ = 2500 studied through simulation and experiment. *Phys. Fluids*, 21, pp. 051702-1 to -4.

Schlichting, H., 1979. *Boundary layer theory, 7th ed.* New York: McGraw-Hill.

Schlichting, H., and K. Gersten, 2000. *Boundary layer theory, 8th revised and enlarged ed.* Springer: Berlin.

Schubauer, G. B., and H. K. Skramstad, 1947. Laminar boundary layer oscillations and stability of laminar flow. *J. Aero. Sci.*, 14, pp. 69-78.

Shehata, A.-M. T. M., 1984. Mean turbulence structure in strongly heated air flows. Ph.D., thesis, U. Arizona.

Shehata, A. M., and D. M. McEligot, 1998. Mean turbulence structure in the viscous layer of strongly-heated internal gas flows. Measurements. *Int. J. Heat Mass Transfer,* 41, pp. 4297-4313.

Smith, C. R., and S. P. Schwartz, 1983. Observation of streamwise rotation in the near-wall region of a turbulent boundary layer. *Phys. Fluids*, 26, pp. 641-652.

Spalart. P. R., 1986. Numerical study of sink-flow boundary layers. J. Fluid Mech., 172, pp. 307-328.

Townsend, A. A., 1951. The structure of the turbulent boundary layer. *Math. Proc., Cambridge Philos. Soc.*, 47, pp. 375-395.

Townsend, A. A., 1961. Equilibrium layers and wall turbulence. *J. Fluid Mech.*, 11, pp. 97-120.

Tuckermann, L. S., M. Chantry and D. Barkley, 2020. Patterns in wall-bounded shear flows. *Ann. Rev. Fluid Mech*, 52, pp. 343-367.

Valentin, F. I., N. Artoun, M. Kawaji and D. M. McEligot, 2018. Experimental study of mixed convection heat transfer at high pressure and high temperature in a graphite flow channel. *J. Heat Transfer,* 140, pp.122502-1 to -10.

von Karman, T., 1939. The analogy between fluid friction and heat transfer. *Trans., ASME*, 61, pp. 705-710.

Walsh, E. J., D. H. Hernon, D. M. McEligot, M. R. D. Davies and A. Bejan, 2006. Application of constructal theory to prediction of boundary layer transition onset. Paper GT2006-91166, ASME Turbo Expo 2006, Barcelona, May.

Weller, H. G., G. Tabor, H. Jasak and C. Fureby, 1998. A tensorial approach to computational continuum mechanics using object-oriented techniques. *Computers in Physics*, 12 (6), pp. 620-

631.

Wood, D. H., 1980. A reattaching, turbulent thin shear layer. Ph.D. thesis, Imperial College, London.

Worsoe-Schmidt, P. M., 1966. Heat transfer and friction for laminar flow of helium and carbon dioxide in a circular tube at high heating rate. *Int. J. Heat Mass Transfer*, 9, pp. 1291-1295.

Worsoe-Schmidt, P. M., and G. Leppert, 1965. Heat transfer and friction for laminar flow of a gas in a circular tube at high heating rate. *Int. J. Heat Mass Transfer*, 8, pp. 1281-1301.